# Numerical Modeling of Flow across the Hollow Fiber Membrane Module of Binary Gas Mixture

**Salman Qadir**

MS Chemical Engineering

00000117574

**School of Chemical and Materials Engineering (SCME)**

**National University of Sciences and Technology (NUST)**

# Numerical Modeling of Flow across the Hollow Fiber Membrane Module of Binary Gas Mixture

**Salman Qadir**

**00000117574**

**This work is submitted as an MS thesis in partial fulfilment of the requirement for the degree of**

**(M.S in Chemical Engineering)**

**Supervisor Name: Dr Arshad Hussain**

**School of Chemical and Materials Engineering (SCME)**

**National University of Sciences and Technology (NUST)**

# DEDICATION

*This thesis is dedicated to my Father Mr. Abdul Qadir (Late) and my Family.*

**Acknowledgments**

Praise is because of ALLAH whose value can't be depicted by speakers, whose bounties can't be checked by mini-computers, whom the tallness of scholarly mettle can't acknowledge, and the diving's of comprehension can't achieve; He for whose portrayal no restriction has been set out, no tribute exists, no time is appointed and no term is settled. Countless acknowledgements upon **"HOLY PROPHET HAZRAT MUHAMMAD (S.A.W.W.)".**

I would like to acknowledge and express my sincere gratitude to my research **supervisor, Dr. Arsahd Hussain** for his infinite care, supervision and friendly guidance to steer me in the right direction. I also would like to thanks to my GEC Members Dr. Muhammad Ahsan and Dr. Iftikhar Ahmad Salarzai for their kindness.

In the end, I must express my very deep gratitude to my parents and friends for providing me with consistent support and continuous inspiration throughout my years of study and through the process of researching and writing this thesis. This accomplishment would not have been possible without them.

Last, I would like to thank for my all MS colleagues being with me through this good period, helping me throughout my research.

*Salman Qadir*

## Abstract

Computational fluid dynamics is applied in membranes modules to study the mass transport and flux for separation of the binary mixture. In the present study, computational fluid dynamics modeling is performed to check the concentration polarization phenomena for binary gas mixture in particular membrane modules. The three-dimensional membrane modules have been considered for finding the mass flux and parametric study to obtain the flow profiles. The membrane model is defined in software for using the permeabilities of asymmetric membranes for gas separation. The membrane is considered as a thin diffusion barrier which has a corresponding thickness to separate the binary gas mixture. CFD allows changing the specification of membrane module to finds the different parameters of the module. Fick's law is used to find the mass flux in all membrane modules and required less slight computational requirements. Cross-flow and counter-current membrane model is applied for flow pattern in all membrane modules. Different gas mixture like $O_2/N_2$, $CO_2/CH_4$, CH4/$CO_2$ and $CH_4/C_2H_6$ is used in a hollow fiber, spiral wound, tubular and flat sheet membrane module. The different parameters of membrane modules like feed pressure permeate pressure, membrane thickness, module length and feed concentration has investigated for finding flow profiles and diffusive fluxes. The results show that concentration polarization has negligible effect on the performance of membrane modules performance for gas separation. The obtained results have been compared with the experimental and verify the performed simulations for different module configurations.

# Table of Contents

# List of Figures

# Table of Figures

# Chapter 1

# 1 Introduction

Membrane gas separation has the ability to remove uncertain species from a gas mixture and membrane allows only one component to pass through the membrane from the mixture because of its selectivity [1]. Membrane gas separation has become traditional process due to its reliability, separation performances, and low maintenance and easy operation [2]. However, membrane technology is being regularly used for separation of various fuel mixtures in different industries due to the economic competitiveness of the present separation technology and demanding situations of competitive environments [3]. Membrane gas separation is primarily used in industries such as for hydrogen recovery from ammonia, hydrogen recovery in refineries, air separation for oxygen purification, sour gas treating and carbon dioxide removal from natural gas [4].

The membrane-based process is driven by the pressure difference in major industries. These processes are integrated with big industrial units but the scenarios for different units are limitless. It is estimated that growth of membrane gas separation will widely increase in 2020 [5]. It is important fact that usage of membrane gas separation technology will decrease the cost of unit operation for gas separation and reduce the environmental hazards. Due to low energy requirements and membrane configurations, membrane separation processes are competent in all practical industrial application. The broad range of membrane materials and continuous research has opened door for various new applications in many industries.

The major development in membrane technology is focused on the membrane materials to achieve a high permeability and selectivity's for best gas separation applications [6]. Mathematical modeling of the membrane gas separation is the latest technology that gives the feasible results of membrane unit design and also gives

parametric studies on the operating condition to make separation process economically viable [7].

In last 30 years, membrane gas separation has become an important part of industrial operation units. A new era of membrane gas separation was started when the Thomas Graham, who developed a method to describe the permeation of gases [8, 9]. Graham proposed a solution-diffusion method which works only with porous membranes [1]. The first industrial unit of membrane-based gas separation was developed by Knoxville and was largest plant of that time. This unit operation has no long-term influence on the development of gas separation processes [10].

Graham gave a significant method for membrane gas separation in which diffusion occurs with the mass transport due to presence of concentration gradient. But this work was identified by Loeb and Sourirajan who developed an asymmetric high flux membrane for RO systems [10, 11]. Monsanto chemical company developed a pilot plant for the separation of hydrogen from ammonia purge gas before product synthesis [11, 12].

More interest was developed in membrane technology and many researchers extended the process of membrane gas separation for carbon dioxide removal from natural gas. In 1980's synthetic membranes were developed to achieve the high permeability and selectivity [13]. These improvements in membrane separation materials with high selectivities made it much competitive. Currently, the membrane technology plays a vital role in industrial applications globally [14].

### 1.1 Membrane and its Mechanism

A membrane is a thin film of polymeric solid which is a semipermeable barrier that restricts the motion of certain species. The rate of transport through membrane gives a separation of certain species and second product species concentrated on the other side. The transport through the membrane due to concentration gradient and pressure gradient [15]. There are several types of membrane i.e. natural, synthetic, symmetric and asymmetric membranes. Natural membranes are based on the natural things that are presents in living organisms i.e. cell membrane. While, synthetic membranes are made of different polymer to achieve the separation of different species because of polymers porous structure [16].

Another classification of the membrane is based on the nature of structure and morphology. The symmetric membrane consists of uniform structure throughout the membrane while asymmetric membranes are different in nature because of small membrane layer with a porous layer. Through a membrane process the feed stream is divided into reject and permeate; permeate is the species allowed to pass through the membrane while reject does not pass through the membrane. The schematic diagram of membrane process is given below [12].

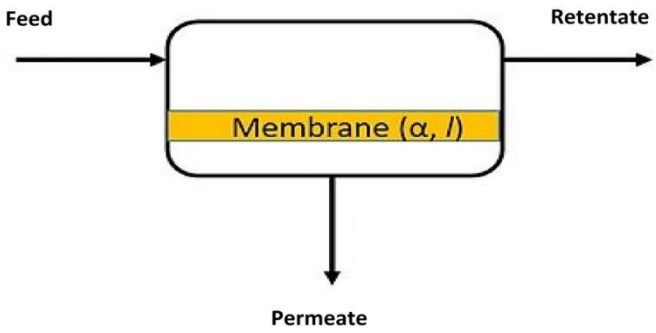


Figure 1 : Membrane process

**1.2 Theory of Gas transport**

The gas transport through the membrane depends on the chemical and physical properties of the polymer. The relation between the membrane, permeate and nature depends on nature of gas molecules, shape and size. Convective flow, molecular sieving and Knudsen diffusion are three cotogories of mechanisms for porous membranes. In dense membranes, the solution-diffusion model is applicable for transport of gas through membranes.

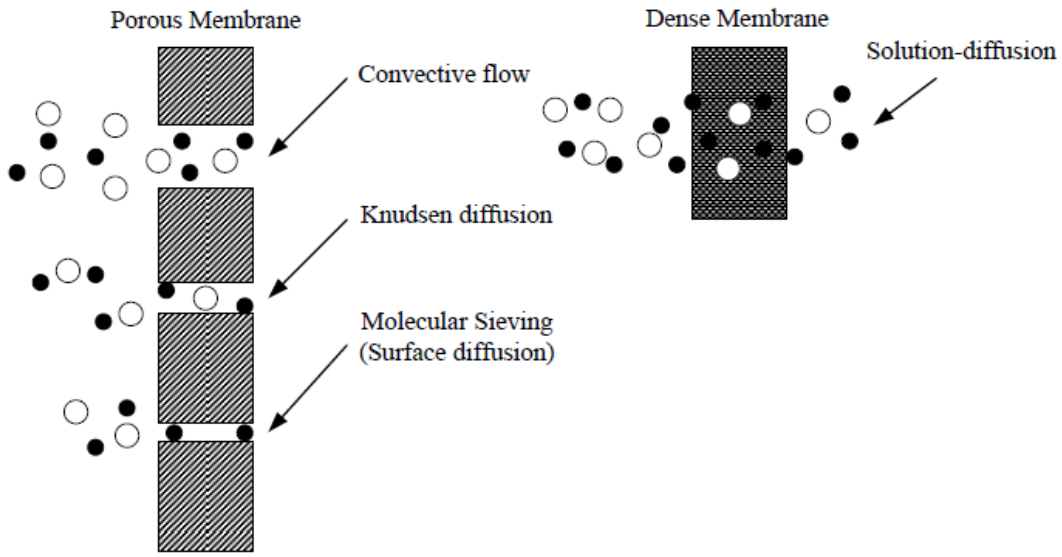


Figure 2 : Theory of gas transport for porous and dense membranes

When the pore size of membrane is decreased the separation occurs with molecular sieving. The gas transport in these membranes is relatively more difficult as first the gas is absorbed and then diffusion takes place. These membranes are not used on commercial scale. But ceramic and glass membranes with high selectivity have been synthesized on lab scale for same size gas molecules [17].

The separation through all commercial dense membranes is based on solution-diffusion model. According to Graham, transport through dense membranes occurs in three steps. In this model, the feed gas from high-pressure side diffuses in the low-pressure side. Both desorption and sorption occur at the interface. The polymer surface is used as an equilibrium between gas phases on both side of the membrane. The permeate can be separated due to the gradient of solubility and diffusivity.

The Flux through the membrane is defined by Fick's Law.

$$F = -D\frac{dC}{dx} \qquad 1.1$$

The concentration at feed side interface of component is defined by Henry Law

$$C = Sp \qquad 1.2$$

Combine the equation 1 and 2 and that gives the flux through the membrane for gas transport

$$F = -SD\frac{\Delta p}{t} \qquad 1.3$$

$$P = DS \qquad 1.4$$

The permeability of the membrane is defined as P.

Putt equation 3 into 4

$$F = -P\frac{\Delta \mathrm{p}}{\mathrm{t}} \qquad 1.5$$

The ability of polymeric membrane that can separate two gases i.e. i and j due to their permeability's ratio $\alpha_{ij}$ is called membrane selectivity.

$$\alpha_{ij} = \frac{P_i}{P_j} = \left[\frac{D_i}{D_j}\right]\left[\frac{S_i}{S_j}\right] \qquad 1.6$$

The $(P_i/P_j)$ is ratio between diffusion coefficients called as mobility selectivity that reveals the permeating molecules have different sizes. While the ratio of $(S_i/S_j)$ is called solubility selectivity that shows two gases have relative condensabilities.

### 1.3 Membrane materials

The membrane material is an important factor for the gas separation because all gases never pass through every material. The selection of membrane material depends on its chemical and physical properties for gas separation.

The membrane can be synthesized under specific conditions to separation certain gas mixtures. The membrane separation performance can be determined on the basis of:

1. Membrane material
2. Thickness and structure of membrane
3. Shape of the membrane
4. Module and Design

The economics of membrane-based gas separation process depends on the permeability and selectivity. For gas separation, a high number of polymer materials have been synthesized.

In refineries and petrochemical industries, the feed stream contains heavy hydrocarbons that create a big problem for separation. When $CO_2$ and hydrocarbons are exposed to polymers, the polymer is swollen, and membrane performance is affected.

The in inorganic membranes and carbon sieve molecular membranes are very attractive because of their high temperature resistance and they can survive with violent chemicals. But, they have many disadvantages too like high cost, brittleness, low permeability for highly dense membranes and low membrane area to volume [6]. Some of the membrane materials are given in Table 1.

**Table 1: Membranes used for gas separation**

| Rubbery Polymers | Glassy Polymers |
|---|---|
| Poly dimethylsiloxane | Cellulose acetate |
| Ethylene Oxide | Polyperfluorodioxoles |
| Propylene Oxide-amide copolymer | Polycarbonates |
| | Polyimides |
| | Polysulfone |

### 1.3 Types of Membrane Modules

The membrane module configuration and feasibility of process is based on the active area of the membrane for separation. In 1960's and 1970's, the membrane modules were commercialized due to decreasing cost. One of the module type is tubular and plate and frames, that design depends on simple filtration technology. Due to their high cost and less membrane area for separation they have been replaced with hollow fiber and spiral wound membrane modules.

#### 1.3.1 Flat Sheet Membrane Module

The flat sheet membrane module is just like flat sheet placed in the rectangular or cylindrical shell. The module is basically used for gas separation for lab scale purposes. The earliest types of membrane systems are Plate-and-frame module and the design is based on a conventional filter press. The comparatively high production cost (as compared to others membrane modules) and leaks caused by the numerous gasket seals in the system have restricted the usage of this system to the small-scale application. Plate-and-frame is also use for electrodialysis and evaporation systems. The schematic diagram of plate-and-frame membrane module is given in Figure 3.

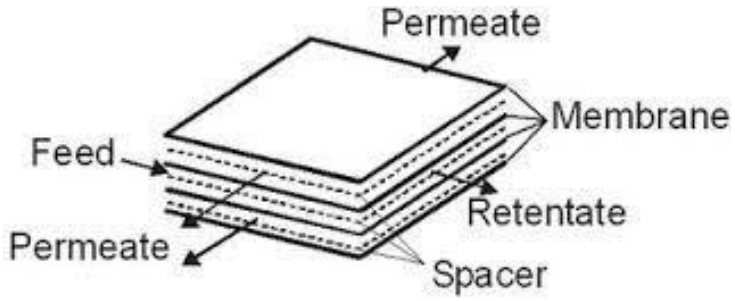


Figure 3: Flat-Plate Membrane Module

### 1.3.2 Tubular Module

The tubular module are tube like structures with porous walls. They work through tangential cross-flow. These tubes are basically made up of polyester or polypropylene which are non-woven fabric and the diameter range of tubes is usually 5 to 25 mm. Two most common housing systems for the tubular modules are supported and unsupported tubes system housing. In the first type, the membrane is placed on the stainless-steel tube while in supported housing system, bundles of tubes are fixed in a vessel and permeate is collected at the end of the vessel.

The unsupported housing system only consists of a substrate tube on which membrane is placed and the casing is made of epoxy resin in which bundles of tubes are present. But mainly these designs offer less capital cost and also decrease the temperature, pressure and pH tolerance.

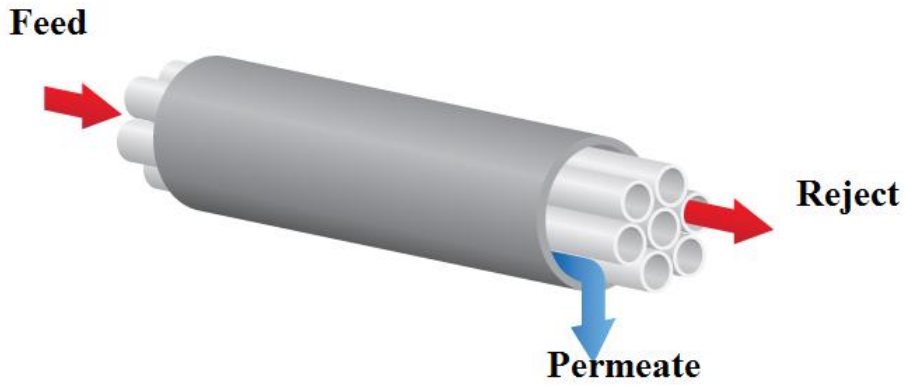


Figure 4: Tubular Membrane Module

### 1.3.4 Hollow fiber Membrane Module

The hollow fiber membrane module consists of large number of fibers in a shell having very small diameter of tubes. The diameter ranges from micrometres with

inside diameter of 200-500 µm meter and the outer diameter of 250-1000 µm. The basic geometry of module is like shell and tube heat exchanger in which thousands of fiber tubes bundle together and the shell is placed as a casing with a diameter of 0.1 to 2.0 meter. The main advantage of this module is the ratio of membrane area with module volume up to 10000 $m^2/m^3$.

Hollow fiber membranes generally have two geometries i.e. shell-side feed and bore side feed. Shell-side feed consists of fibers in a close bundle within a pressure vessel. Pressure is created from the shell-side while permeation occurs through the fiber wall. However, reject passes through open fiber ends. The design allows the large surface area of membrane material to be compactly enclosed in an economically viable system. The fiber has small diameters and the wall has high thickness because of large pressure requirement. Feed side hollow fiber is shown in Figure 5. Fibers are of open ends and feed fluid circulates through the bore of fibers.

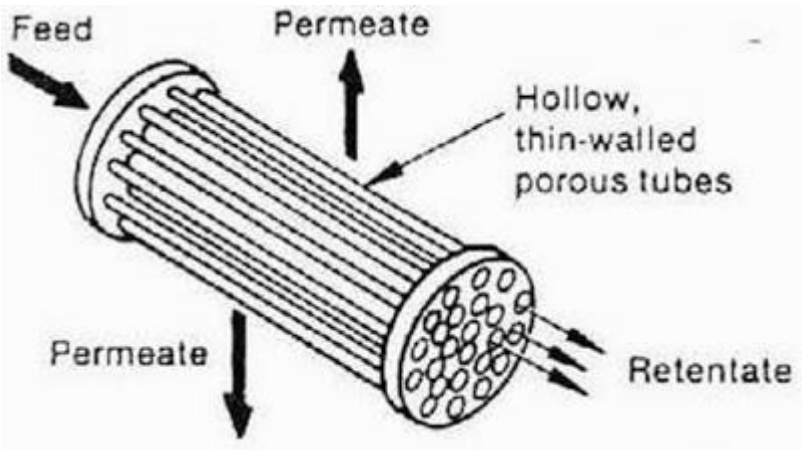


Figure 5: Hollow Fiber Membrane Module

### 1.3.5 Spiral wound membrane module

The spiral wound membrane modules consist of three flat sheets in which one centre plate is used as a membrane and all plates are wrapped around the center tube. The centre tube is used for collecting permeate that passes through the membrane. This design of spiral wound membrane module is simply retained flat membranes while increasing the area of membrane per unit volume upto 330 $m^2/m^3$. The diameter of the spiral wound is 100 mm to 200 mm and its axial length is 1 to 1.5 m. The dimensions of the flat sheet are 1-2 m by 2-3 m and spacing between membranes is 1 mm.

The spiral wound membrane module is placed in a solid metal shell casing. The feed gas enters through the shell side and gas flows in the spiral direction of the chamber. The feed gas passing through the membrane is collected in a permeate channel and permeate flows in the direction perpendicular to the membrane and the permeate is collected in a perforated tube at the end.

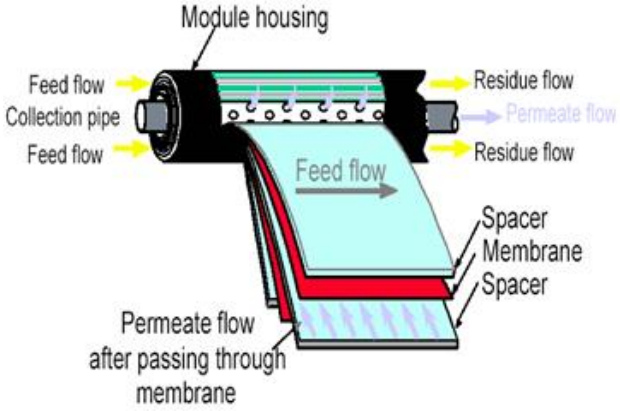


Figure 6: Spiral wound membrane module

### 1.4 Industrial application of membrane gas separation

The main industrial applications of membrane gas separation technology are still rising and developing. Many industrial plants i.e Air Liquids, Air Products (Perma) and Praxair are using membrane units. Furthermore, plants developing membrane systems for the natural gas purifications. The list of industrial application for membrane gas separation is given in the table 2.

Table 2 : Industrial application of membrane gas separation

| **Separation** | **Process** |
|---|---|
| $H_2/N_2$ | Ammonia Purge gas unit |
| $H_2/CO$ | Syngas ratio adjustment |
| $O_2/N_2$ | $N_2$ Production |
| $CO_2/N_2/O_2$ | $CO_2$ removal from flue gas |
| $H_2S$/hydrocarbons | Sour gas treating |
| He/Hydrocarbons | Helium separation |

| | |
|---|---|
| $He/N_2$ | Helium recovery |
| Air/Hydrocarbons | Pollution Control |
| Volatile organic species | Polyolefin purge gas purification |

# Chapter-2

# 2 Literature Review

Natural gas is considered as one of the significant fossil fuel. It is found in subsurface reservoirs and mostly produced as the byproduct of oil production. The demand for natural gas has seen a significant rise in recent years. As per the reports of EIA (U.S. Energy Information Administration), the global natural gas consumption is increasing 4% annually. It is estimated that 10% of world power sector depends on natural gas. By 2040, the power production and industrial usage are expected to depend 73% on natural gas. Natural gas consists of several chemical species including methane, ethane, propane, butane, water vapour, nitrogen and acid gases such as carbon dioxide ($CO_2$) and hydrogen sulfide ($H_2S$). Out of the species comprising natural gas $CO_2$, $N_2$, water vapour and $H_2S$ are considered as impurities. The concentration of impurities in natural ranges from 4-50% depending upon the reservoir it is produced from. The presence of these impurities can significantly affect pipelines such as corrosion and raise health and safety concerns too. Therefore, typical pipeline specifications usually mandate the concentration of carbon dioxide in natural gas to not exceed 2–5 volume percent, Therefore, making it necessary to treat the natural gas and remove the impurities before it is transported for the commercial or industrial use. To remove the impurities from natural gas several methods are used in the industry such as amine treatment. In recent years membrane separation process has also been widely used as it is more economical compared to the other processes. In the membrane processes for acid gas removal hollow fiber membranes and reverse osmosis membrane separation process is implied**.** However, there are various types of design for reverse osmosis membrane modules such as spiral wound membrane and hollow fiber membrane modules. Hollow fiber membrane modules can be designed with the cross flow or parallel flow configurations.

There are several research studies to study flow characteristics in gas separation modules. Few studies considered spacers in the feed channels to promote momentum mixing and support membranes. Saeed  investigated flow structures in a feed channel

containing spacer with different spacing and arrangement [18]. Saeed and his co-workers considered a three-dimensional feed channel in their study. Their study demonstrated that the mass transfer coefficient remains similar in all cases even though the magnitude of shear stress along the surface of membrane differs. Mojab conducted numerical and experimental studies to examine flow profiles in a feed channel filled with spacers and surrounded by spiral-wound membranes [19]. They conducted transient simulations by utilizing turbulence model for a range of Reynolds number from 100 to 1000. Shakaib investigated the effect of spacers in a spiral wound membrane module [20]. Their study concluded that geometrical parameter of spacers like thickness and the angle of attack influences the level of wall shear rates and the mass transfer coefficient. While Koutsou introduced a novel reject-spacer design in order to eliminate the "dead-flow" zones that cause a reduction in mass transfer [21]. Karod investigated the effect of the arrangement of spacers on pressure drop in a rectangular channel bounded by membranes. They reported that the uniform shear rate along the surface of membranes and high-pressure drop across the channel was observed when using the symmetric spacers [22]. Fimbres-Weihs investigated effects of a spacer configuration and the flow rate of the pressure drop and the mass transfer coefficient. By using an empirical co-relation to calculate mass transfer coefficient the membrane wall was treated as the impermeable surface [23]. Vinther modeled the hollow fiber membrane for ultrafiltration process [24]. Marocs performed a transient simulation for a 2D model of hollow fiber membrane in an ultrafiltration system. Their results showed that the pressure drop significantly influences the concentration polarization in hollow fiber membrane module [25]. Anqi conducted a three-dimensional computational study for a desalination process over a wide range of flow rates. Their results showed that the membrane performance is better at higher flow rates and the arrangement of spacers influences the membrane performance significantly [2]. Alkhamis introduced a new mass flux model for reverse osmosis membrane module for gas separation. The mass flux is calculated on the basis of the local pressure, concentration, permeability, and selectivity of the membrane [26]. They also studied the flow and mass transport in spiral wound membrane module containing spacers and concluded that the spacers enhance the membrane function. Alrehili conducted computational fluid dynamics for a binary mixture of $CO_2$ and $CH_4$ [27]. The hollow fiber studied by them included a bank of hollow fiber membrane with two different arrangements

i.e. an inline and a staggered. The membrane surface was treated as a functional surface where the mass flux and concentration of species are calculated as a function of particle pressure, membrane permeability, and selectivity. Their studies demonstrated that the in cross-flow configuration a better mixing is achieved resulting in enhanced membrane flux performance and improved overall performance. Furthermore, they proved that staggered arrangements perform better than inline arrangements.

### 2.1 Problem Statement

The membrane gas separation is an efficient technique which is used to separate the gaseous mixtures to obtain a maximum purity of gas. The membrane-based gas separation performance depends on the concentration polarization.

The concentration polarization occurs during gas separation due to the presence of gradient of concentration in the membrane with solution interface. The transfer of some species through the membrane is because of membrane permeability, which restricts some species in upstream/feed stream and are concentrated at membrane surface while the transfer of permeate species through the membrane is decreased. This phenomenon is called the concentration polarization in membranes.

Now, the present problem is discussed in major membrane modules to show the gas variations in feed side and permeate side. The Computational fluid dynamics is applied to study the flow profiles of gases in membrane modules. Different membrane parameters like permeability, feed pressure, permeate pressure and feed gas concentration have been discussed here. The membrane is defined as a thin diffusion barrier which allows passing of only a certain gas species.

### 2.2 Objectives

The objectives of this study are;

1. To Design a membrane model in COMSOL Software.
2. To Design all membrane modules for gas separation.
3. To investigate different membrane parameters such as feed pressure, feed gas concentration and module length.
4. Validation of simulated results with literature and experimental results.

## 2.3 Thesis Management

Chapter 1 describes the introduction, problem statement, and objectives of the research. Literature survey related to CFD simulations of membrane modules is discussed in chapter 2. Chapter 3 describes the mathematical modeling of the membrane for separation of the binary gas mixture. Chapter 4 describes the membrane geometry formation and meshing of modules. Chapter 5 represents all CFD results of membranes modules for gas separation and discussed the results validations. Chapter 6 describes the conclusions of the thesis and also future recommendations.

# Chapter 3

# 3 Mathematical Modeling

Computational fluid dynamics deals with a set of the partial differential equation which is based on mass, momentum and heat transport. CFD is a very useful technique for simulation of any system at lab scale or industrial scale. CFD tool is applied to simulate the model to understand the fluid dynamics with changing different parameters.

### 3.1 Convection and Diffusion

In chemical engineering mode, the convection and diffusion model is applicable for mass transport which is described by the Fick's Law. In the 19$^{th}$ century, Fick gave the simplest definition of diffusion for a mass transport. The mass flux of any species is directly proportional to concentration gradient due to diffusion. The rate of change of concentration at a point in space is proportional to the second derivative of concentration with space.

### 3.2 Mathematical Modeling of Mass Transport

The transport of diluted species for chemical engineering modules provides an environment for the modeling of mass transport in a chemical species. Here, the diluted species interface model is applied, which shows all species present in a diluted form. When dilution model is applied it shows that the properties of solute are same as a present solvent. Fick's law also defines solution diffusion in a mixture. The transport of dilute species provides both convection and diffusion models for simulation in all dimensions.

### 3.3 Convection and Diffusion Model

In convection and diffusion model, the mass transport equation contains both phenomena occurrs simultaneously. The mass balance equation is

$$\frac{\partial C}{\partial t} + \nabla \cdot (-D_i \nabla C_i + C_i \cdot u) = R_i \quad (1)$$

Here, $C_i$ = Concentration of any species i in mol/m$^3$.

$D_i$ = Diffusion coefficient in m$^2$/s.

$R_i$ = Rate of reaction for any specie i in mol/($m^3$.s).

The convective transport accounts for the bulk flow of fluid due to velocity u. This term u can be solved analytically or solving these phenomenon by coupling the momentum equation with the mass balance equation. These all expressions which includes time, spatial and velocity component variables are used for mass balance with convection.

The right-hand side of mass balance equation represents a diffusion mechanism which deals with the diluted and solvent species. The nebula operators show three directions of space variables in x, y and z-direction. Finally, the source term is on the right side of the equation that shows a chemical reaction occurring in the process. When source term is specified then the reaction node must show a specific equation of reaction.

### 3.4 Diffusion Term

The chemical species are transferred from high region to low region due to diffusion that becomes mass transfer phenomena with time and space. The chemical species are dissolved in a solvent or any gas mixture i.e. oxygen enrichment in the air. The evolution of species' mass transfer is depending on their concentration with respect to time and space. The gradient for diffusion occurs due to the motion of molecules. Due to the kinetic energy of molecules, they collide with each other in random directions. The flux for diffusion can be written as:

$$N_i = -D\nabla . C_i \tag{2}$$

### 3.5 Convective Term

The convection in mass transfer occurs by bulk flow of fluid in space. Due to velocity, both phenomena of convection and diffusion can be incorporated. It means that convection can occur with a velocity of average molecules and diffusion occurs due to concentration difference in a fluid.

The transport of diluted species in which single component acts as carrier gas or solvent that represents the system momentum. The bulk flux can be written as:

$$N_i = C_i . u \tag{3}$$

Where $C_i$ is the concentration of specie i (mol/$m^3$) and $u$ is the velocity (m/s).

### 3.6 Source Term

Source term is defined in terms of rate of reaction R. For transport of diluted species, the chemical reaction is added in the convection and diffusion model. This model is applicable only for chemical reactors and engineering applications.

### 3.7 The Convection and Diffusion Application Mode

The diffusion and convection equation is applicable for mass transfer in the transport of diluted species. The diffusion and convection equation is:

$$\frac{\partial C}{\partial t} + \nabla \cdot (-D_i \nabla C_i + C_i \cdot u) = R_i \quad (4)$$

Where, $C_i$ represents the concentration of species $i$ (M $L^3$), $D_i$ denotes diffusion coefficient ($L^2$ $T^{-1}$), $u$ is the velocity vector (L $T^{-1}$) and $R_i$ shows the reaction term (M $L^3$ $T^{-1}$). The rate of reaction term is expressed in terms of reactants and products. The flux vector expression represents both convection and diffusion in terms of diffusive flux and mass flux.

$$N_i = -D_i \nabla C_i + C_i u \quad (5)$$

Here, $Ni$ is vector mass flux with dimension (M $L^{-2}$ $T^{-1}$). The dissolved species for diffusion coefficient show the interaction between the solvent and the solute. In the Maxwell Stefan equation, the diffusion and convection mode has accounted the interaction of different dissolved species. The boundary condition for mass flux in diffusion and convection mode is expressed as:

$$N_i . n = N_o \quad (6)$$

When the insulation has been applied then the boundary condition is changed to:

$$N_i . n = 0 \quad (7)$$

The boundary condition in the transport of diluted species imposed in terms of concentration.

$$C_i = C_{i,o} \quad (8)$$

The convective flux boundary condition assumes that all mass passing through this boundary is convection-dominated. This first assumes that any mass flux due to diffusion across this boundary is zero:

$$n.(-D_i \nabla C_i) = 0 \quad (9)$$

So that:

$$N_i.n = C_i u.n \quad (10)$$

This is a useful boundary condition, particularly in convection-dominated mass balances where the outlet concentration is unknown.

### 3.8 Mathematical Modeling of Membrane Model

#### 3.8.1 Diffusion of Gas through Membrane

The diffusion is important mechanism which takes place in mass transfer problems. Molecular diffusion only deals with membranes and microporous catalysts and some other thin films. Here, we have focused on the diffusion through membranes for certain chemical species. The system is considered to check the permeability of gases where feed side of gas in one compartment and permeate is passed through a membrane which is called pure gas on another side of the membrane. The concentration of both sides is predicted with the unsteady state to obtain the flux through a membrane with certain permeabilities of gas.

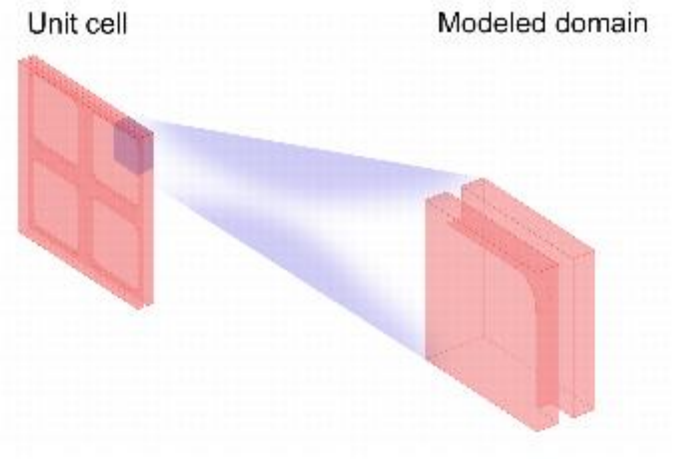


Figure 7: Unit Cell of Membrane Module

The unit cell is a small part of the membrane module that demonstrates the whole membrane module. In this model, we studied the initial flux in the membrane, which corresponds to the largest difference in concentration between the two chambers on different sides of the membrane.

### 3.8.2 MODEL DEFINITION

The steady-state diffusion equation shows the mass transport in model with diffusion.

The model equation for steady-state mass transfer:

$$D\nabla^2 C = 0 \tag{11}$$

Where $C$ denotes concentration (mole/m$^3$) and $D$ the diffusion coefficient of the diffusing species (m$^2$/s). The all boundaries are considered as insulating.

$$D\nabla C.n = 0 \tag{12}$$

The two faces applied as a boundary condition where the concentration of two components set as high to low.

B.C.1:

$$C = C_o \tag{13}$$

B.C.2:

$$C = C_{o,1} \tag{14}$$

Now, the flux through the membrane is calculated as:

$$J = \frac{D}{\delta}(C_o - C_{o,1}) \tag{15}$$

Where, $\frac{D}{\delta}$ is defined as thin diffusion barrier.

The permeability of gas defines the diffusion into Solubility.

We know that

$$D = P/S \tag{16}$$

The solubility of gases is calculated as:

$$S = \frac{\Delta C}{\Delta p} \tag{17}$$

Putt solubility equation into permeability equation

$$D = \frac{P}{(\frac{\Delta C}{\Delta p})} \tag{18}$$

This model is applied to different geometries of membrane modules to check the permeability and flux of gases.

### 3.8.3 Model Geometry

The four main geometries of membrane modules have been configured to find the flow profiles for different mixtures

Figure 8: Geometry of flat sheet membrane module

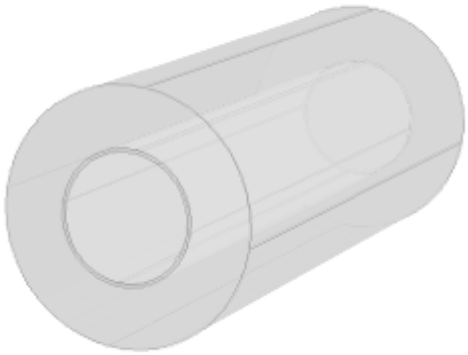

Figure 9: Geometry of tubular membrane module

Figure 10: Geometry of spiral wound membrane module

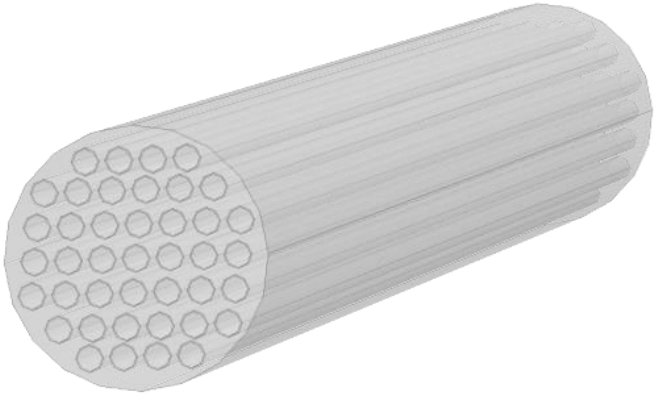

Figure 11: Geometry of hollow fiber membrane module

# Chapter-4

# 4 Results and Discussion

The main objective of present work is to find the flow profiles of different membrane modules i.e. hollow fiber module, spiral wound membrane module, tubular and flat sheet membrane module. The use of different parameters like feed pressure permeate pressure, concentrations across the length, stage cut, permeability and feed concentration have been configured. The work is carried out by using COMSOL Multiphysics software for CFD of different membrane modules. Furthermore, to find the diffusive flux, total flux and concentration variations across the length of all membrane modules.

### 4.1 Hollow Fiber Membrane Module

The hollow fiber membrane module is like a shell-tube heat exchanger geometry in which hundreds of fibers or tubes are placed in a single shell. The module dimensions are taken from the published literature. The conditions are given in the table.

Table 3: Hollow fiber membrane module configuration and specifications [28] .

| Parameters | Units | Values |
|---|---|---|
| Fiber inner diameter | $\mu m$ | 80 |
| Fiber outer diameter | $\mu m$ | 160 |
| Module diameter | $mm$ | 9.5 |
| Active fiber length | $cm$ | 25 |
| Feed mole fraction | ---- | $0.205O_2$ /$0.795N_2$ |
| Feed pressure | $Kpa$ | 790.8 |
| Permeate pressure | $Kpa$ | 101.3 |
| Permeance | $10^{-10}\ mol\ m^{-2}s^{-1}pa^{-1}$ | $30.78O_2$ /$5.7N_2$ |

The simulation of hollow fiber membrane module was performed with variation of feed gas $O_2$ concentration in reject and permeates side. The feed gas enters the membrane module from the fiber-bore side and cross-flow model is used to consider the boundary conditions. The boundary conditions are applied for high feed concentration on inner tube side and low feed concentration on shell side. The thickness of fiber is considered as the membrane, which is a thin diffusion barrier.

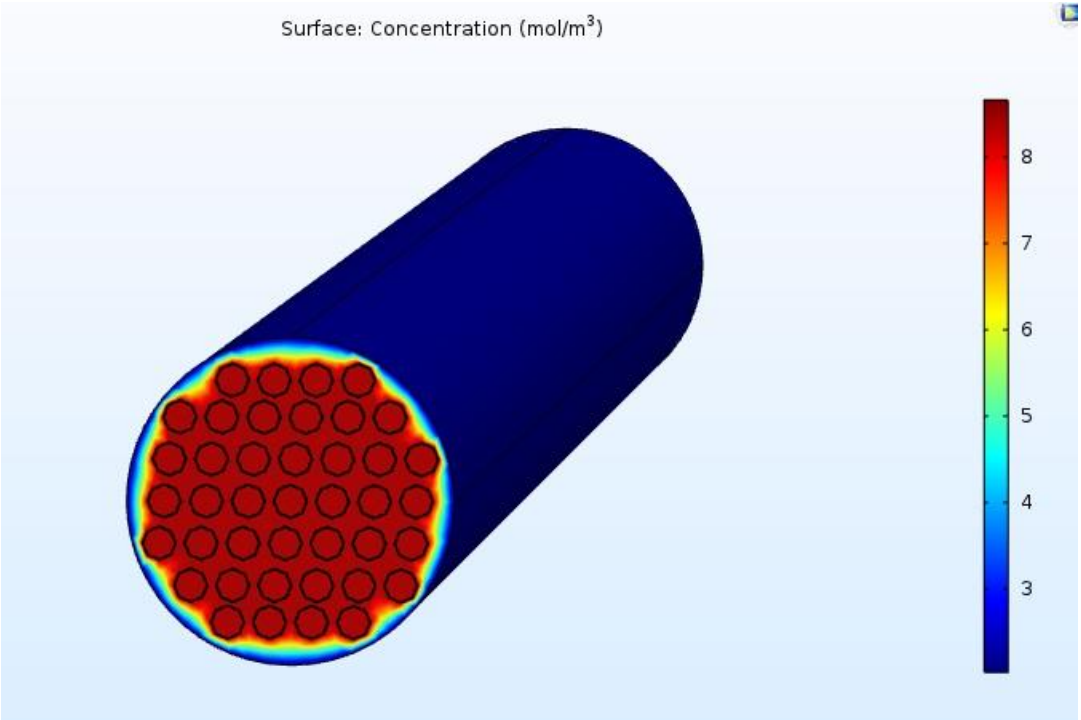


Figure 12: Concentration of feed gas in hollow fiber membrane module

It can be observed in Fig.12 that a concentration of feed to permeate side varies as a cross-flow model. The aims of this study is to check the variation of feed gas between tube and shell side. The concentration is varying in the fibers but is not visually observed, which is shown as the gradient in subsequent section. The concentration variation is not visualized because of the distance between fibers which is in few micrometers.

The concentration of hollow fiber membrane module is also shown in the slice. The colour bar shows the concentration of slice module. The important fact is that contour shows the variation of concentration in the centre of the module. The profile of concentration of oxygen in hollow fiber membrane module can be observed in Fig.13.

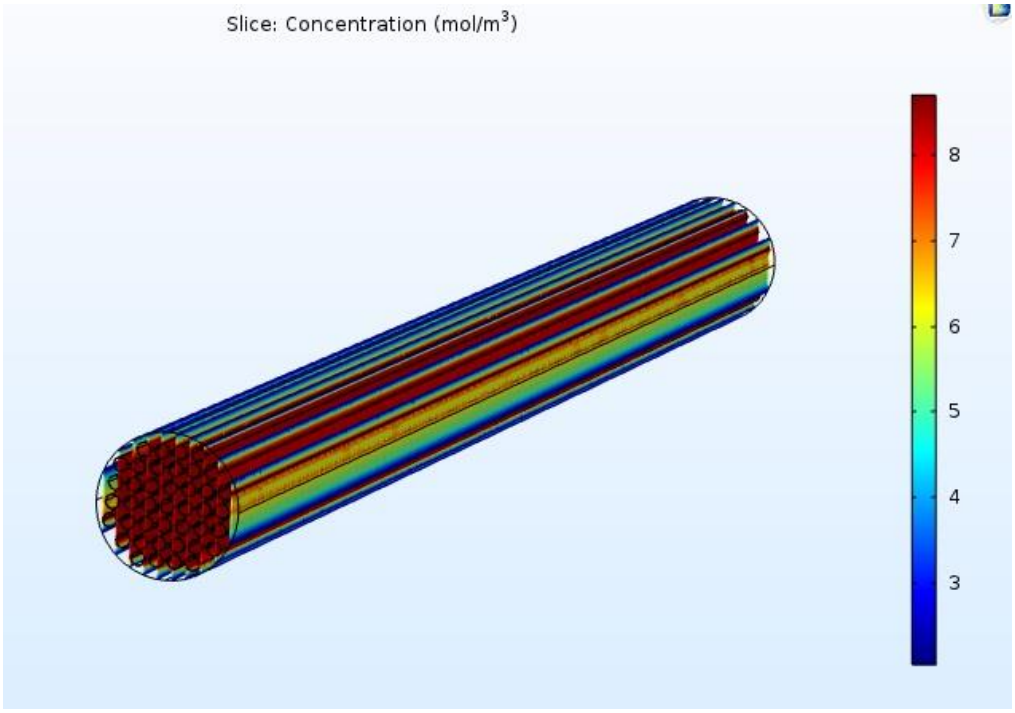


Figure 13: Slice concentration of feed gas in hollow fiber membrane module

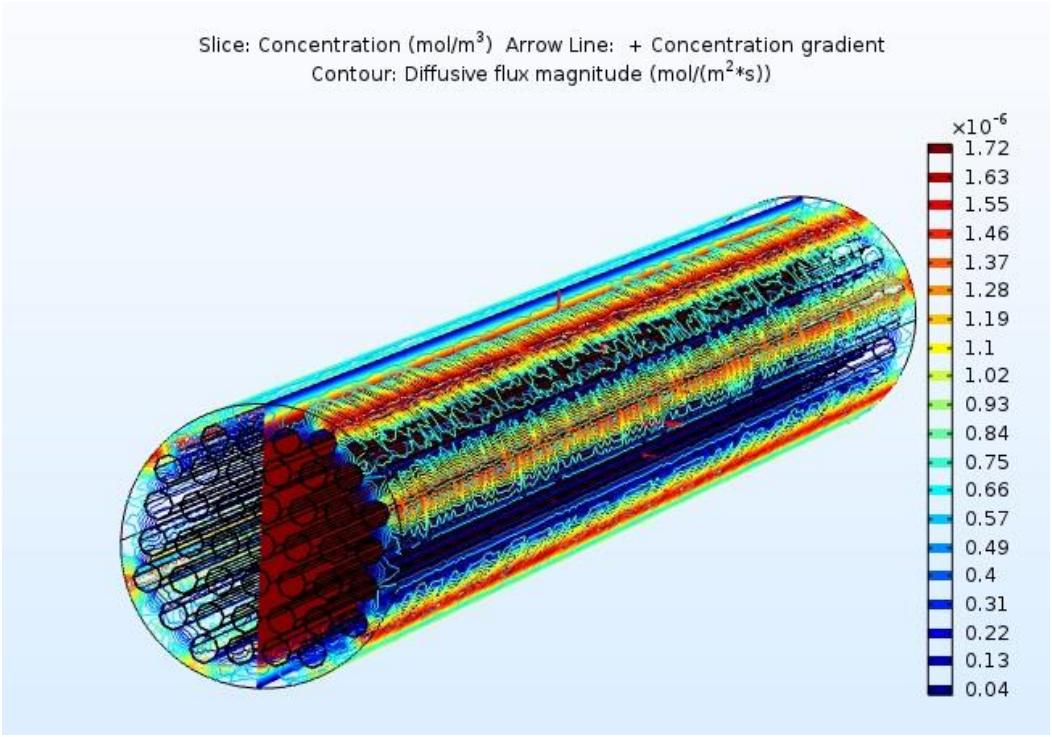


Figure 14: Diffusive flux magnitude in hollow fiber membrane module for oxygen

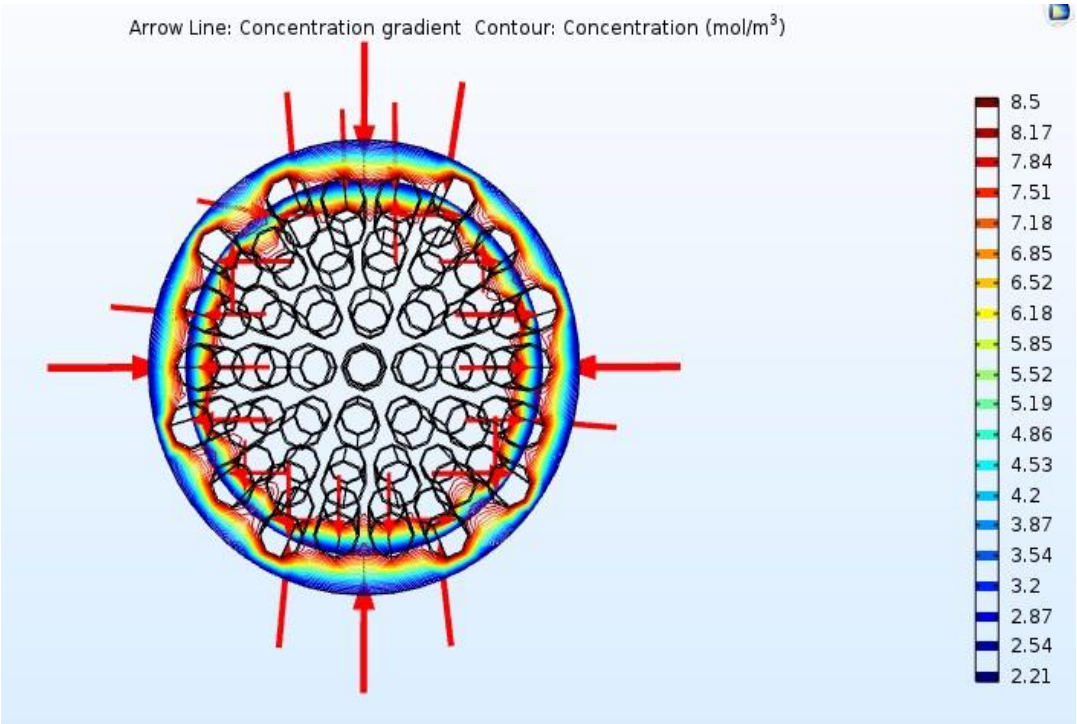


Figure 15: Concentration gradient for hollow fiber membrane module

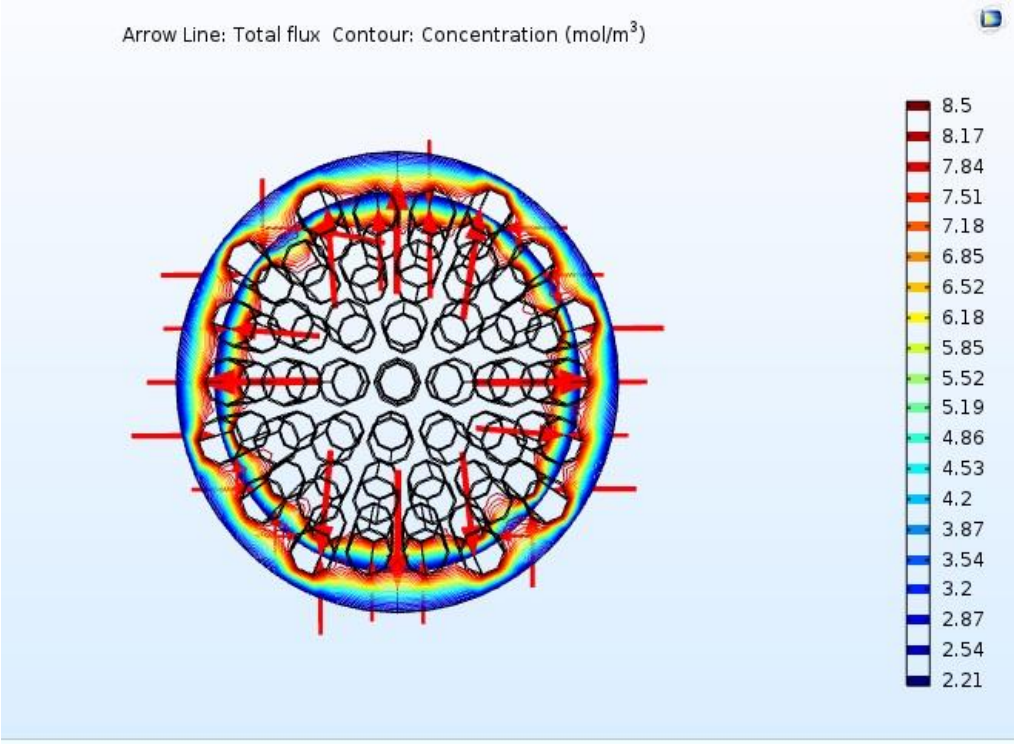


Figure 16: Total flux of hollow fiber membrane module

Fig.14 shows the diffusive flux magnitude in the hollow fiber membrane module. The present result in figure describes the diffusive flux magnitude in the membrane module. The flux can be calculated in a membrane module with given parameter to

the software. The flux can be changed with an increase or decrease the other parameters.

Fig 15 shows the concentration gradient present in the hollow fiber membrane module for oxygen-nitrogen separation. The arrow shows that the gas is diffused through membrane fiber side to the permeate shell side of the module. The results verify that the gradient is present and gas can be passed through the membrane at certain permeability.

The total flux for the separation of oxygen-nitrogen is also discussed in hollow fiber membrane module. Fig.16 shows that the arrow present in contour points the performance of membrane totals flux.

### 4.2 Spiral Wound Membrane Module

The spiral wound membrane module consists of three to four flat sheets which are wrapped around the central perforated tube. These types of membrane modules are used for the separation of decline water and to separate the gaseous mixture. A feed is passed axially across the membrane envelope and permeate goes into membrane envelope then it moves towards the tube side and collecting in the tube.

The $CO_2$/ $CH_4$ separation is considered for the spiral wound membrane module and parameters are obtained from the literature.

Table 4 : Spiral wound membrane module configuration and specifications [29].

| Parameters | Units | Values |
|---|---|---|
| Flow rate | 10 | 10 |
| Feed Pressure | Pa | $35\times10^{5}$ |
| Permeate Pressure | Pa | $1.01325\times10^{5}$ |
| Feed Concentration($CO_2$) | $mol/m^3$ | 20% |
| Outlet Concentration | $mol/m^3$ | Less than 2% |
| Permeability of $CH_4$ | $mol/M.Pa.s.m^2$ | $1.48\times10^{-3}$ |
| Selectivity(CO2/CH4) | ----- | 20 |

The simulation of spiral wound membrane modules is presented to show the concentration of feed gas $CO_2$ in reject and permeate side. The feed gas is entered in the membrane module from central tube and moves throughout at the end. The module result shows that concentration of $CO_2$ changes throughout the module. The high concentration is applied on the first wrapped sheet as a boundary condition, permeate is collected in permeate channel and low concentration is applied on the second plate of the membrane module.

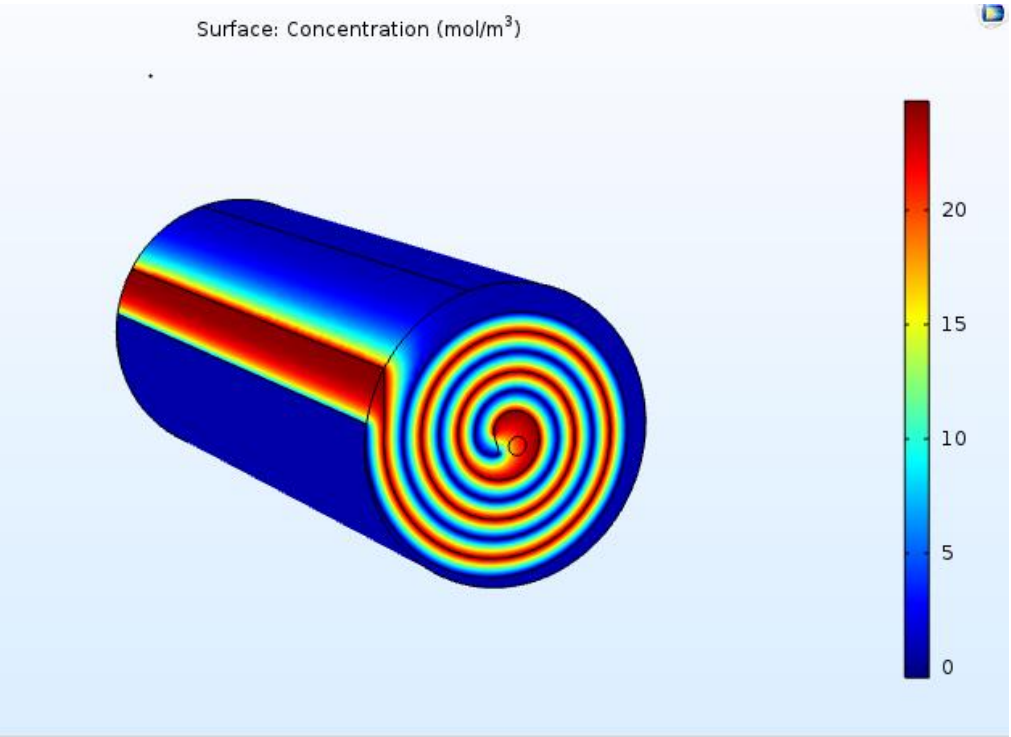


Figure 17: Concentration of $CO_2$ in spiral wound membrane module

The above contour of $CO_2$ gas shows that gas concentration varies along the membrane in permeate and residue side. The bar colour shows the concentration from high to low. The gas entered into tube side then moved through the feed channel which then passed through the membrane and collected in permeate channel.

The concentration of $CO_2$ in spiral wound membrane module is also shown in the slice. The colour bar shows the concentration of slice module. The result verifies the concentration variation in the centre of the module. It verifies that gas diffuses through the membrane from feed channel and collected in the permeate channel. Fig 18 shows the concentration of $CO_2$ as a slice in spiral wound membrane module.

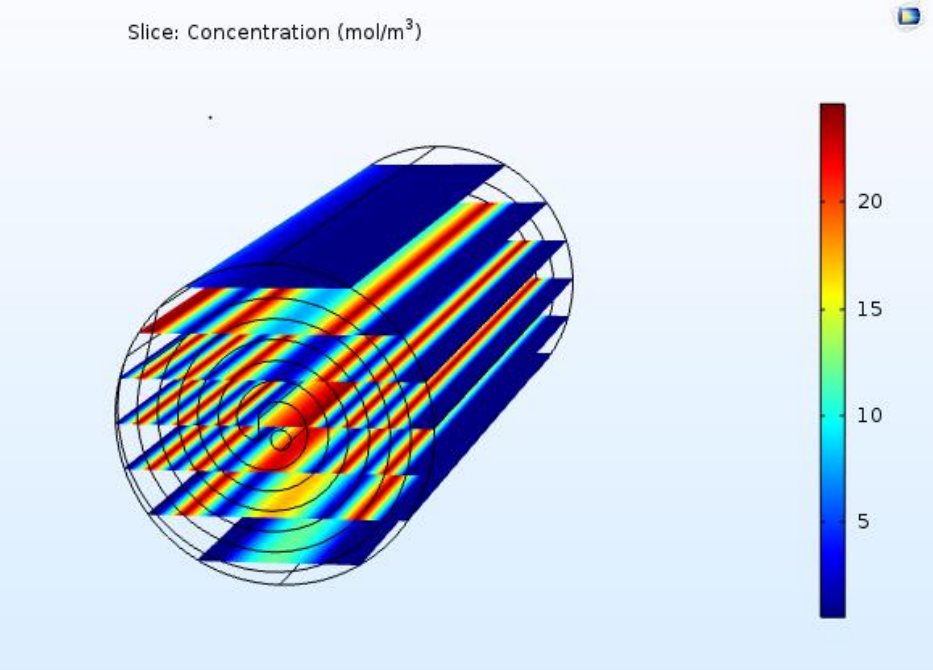


Figure 18: Slice concentration of $CO_2$ in spiral wound membrane module.

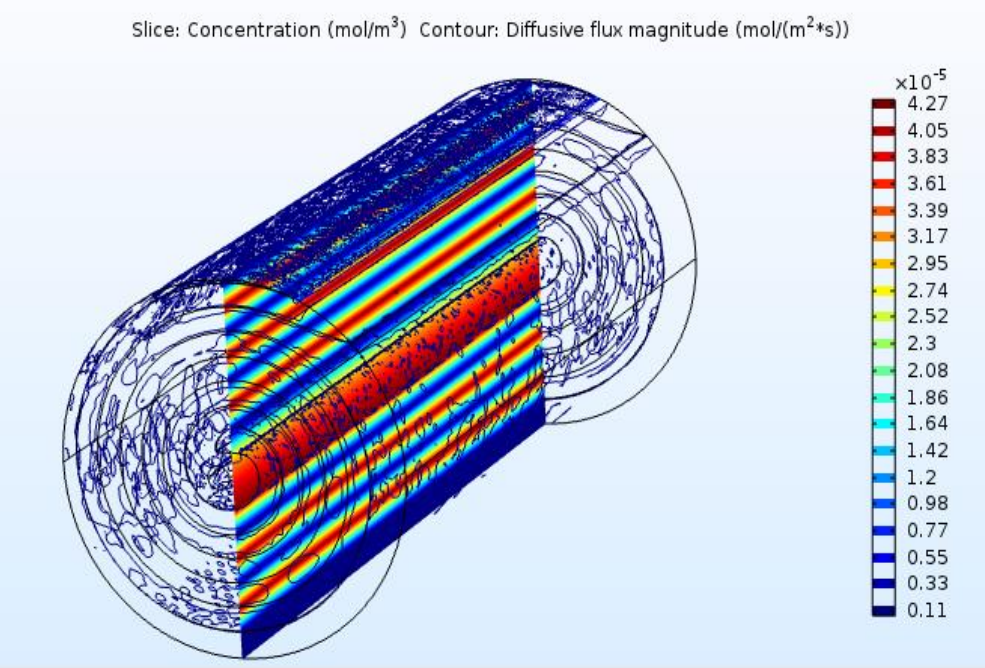


Figure 19: Diffusive flux magnitude in spiral wound membrane module

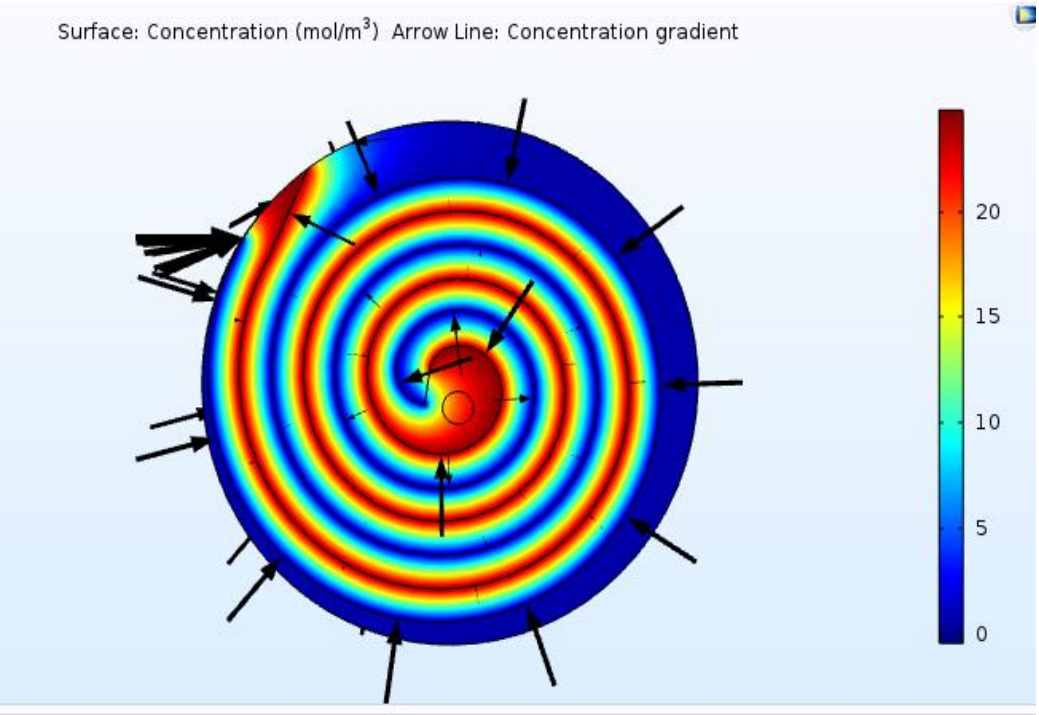


Figure 20 : Concentration gradient in spiral wound membrane module

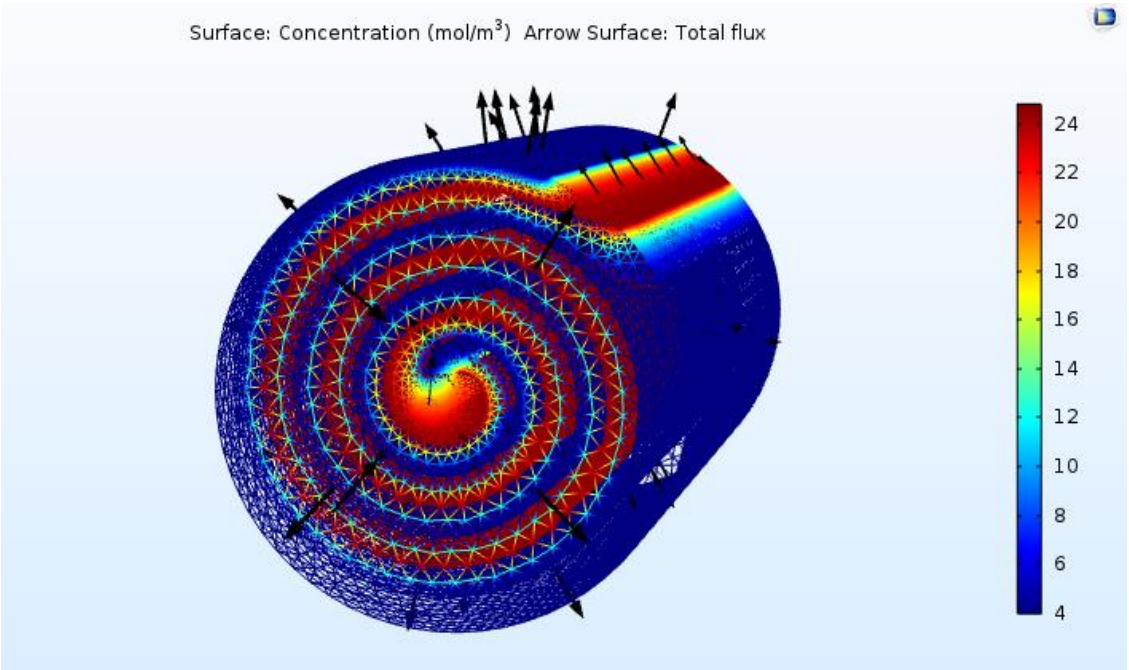


Figure 21: Total Flux in spiral wound membrane module

Fig.19 shows the diffusive flux magnitude in the spiral wound membrane module for $CO_2$. The diffusive flux magnitude in membrane module can be obtained from given parameters like concentrations and permeability. Basically, the flux is calculated in

the module is described by Fick law. It represents that mass transport can occur through the membrane in spiral wound membrane module.

Fig.20 shows that concentration gradient present in the spiral wound membrane module for $CO_2/CH_4$ separation. The important parameter which the arrow shows is the gas passes through feed side to the permeate collector of the module. The results verify that the gradient is present and gas can be diffused through the membrane.

The total flux for the separation of $CO_2/CH_4$ is also discussed in spiral wound membrane module. In Fig.21 the arrow present in contour shows the performance of membrane total flux. The total flux indicates that gas is diffused from high concentration to low concentration side.

Fig.22 shows that the concentration variation from outer plate to inner plate of membrane module which represents the concentration of $CH_4$ is changed in spiral wound membrane module.

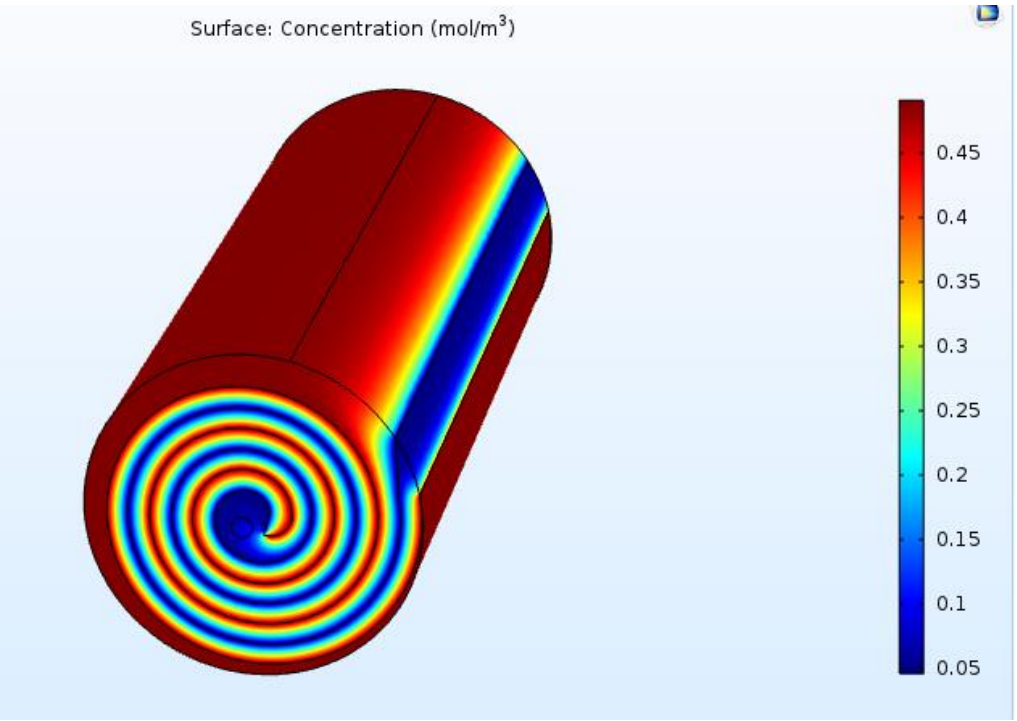


Figure 22: $CH_4$ concentration in spiral wound membrane module

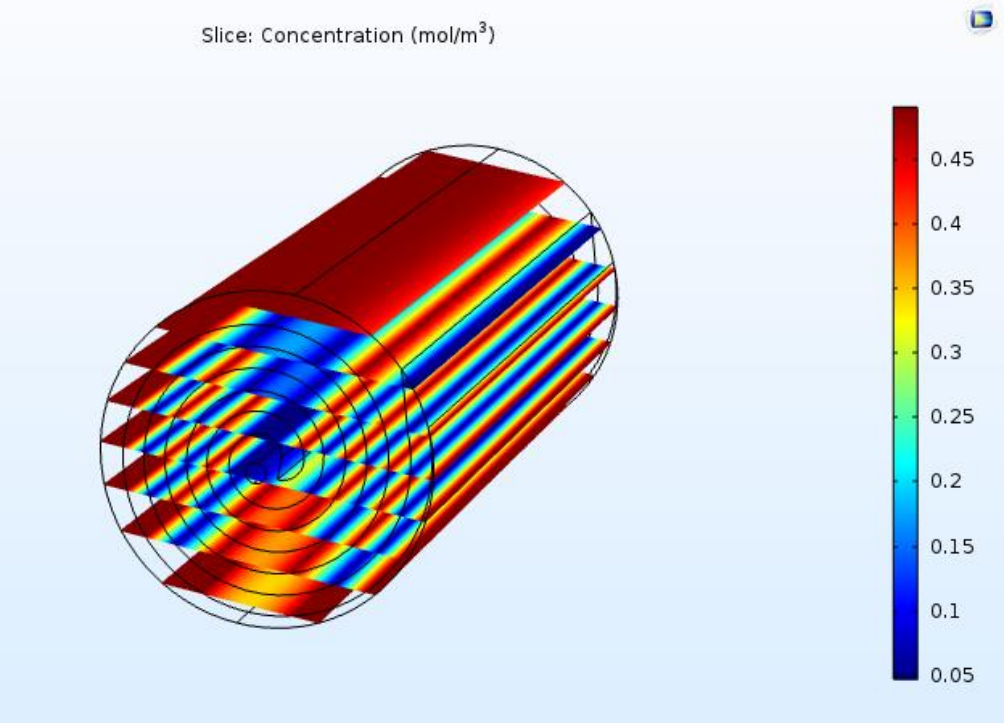


Figure 23: Slice concentration of $CH_4$ in spiral wound membrane module

### 4.3 Tubular Membrane Module

The tubular membrane module geometry consists of 6 to 30 tubes in a single shell but four to six modules are compacted together to form the large surface area. The module dimensions taken from the literature. The conditions are given in the table 5.

Table 5 : Tubular membrane module configuration and specifications [30].

| Parameters | Units | Values |
|---|---|---|
| Outer tube Diameter | *Um* | 400 |
| Outer bundle Diameter | *Cm* | 20 |
| Length of tube | *Cm* | 100 |
| Permeance(For CO2)/ CH4 | *GPu* | 10/0.25 |
| Selectivity | --- | 40 |
| Feed Pressure | *Psia* | 1000 |
| Permeate Pressure | *Psia* | 20 |

The simulation of tubular membrane modules shows that the concentration of feed gas $CO_2$ changes in reject and permeate side. The feed gas entered in the membrane module from tubes. The cross-flow model is applied to consider the boundary conditions. The boundary conditions are applied for high feed concentration on inner tube side and low feed concentration on shell side. The thickness of tube is considered as the membrane, which is a thin diffusion barrier. The concentration of $CO_2$ in tubular membrane modules is given below.

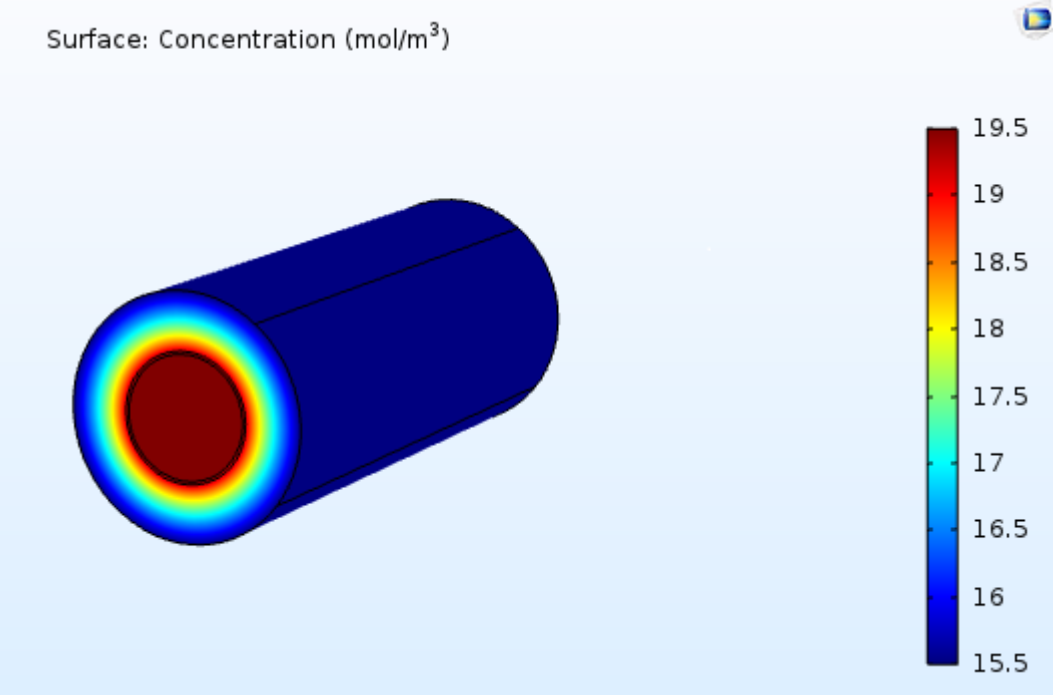


Figure 24: $CO_2$ concentration in tubular membrane module

Fig.24 of tubular membrane module shows a concentration of feed gas in feed and permeates side. The applied model is a cross-flow model for gas separation. The contour tells about the concentration variation of gas between tube and shell side. The concentration of tubes is changed but due to the compactness of module, it is not visually observed.

The concentration of tubular module is also shown in the slice. The colour bar shows the concentration of module in the slice. The present contour tells about the concentration of $CO_2$ in the slice. The contour tells us about the feed gas variations in the feed and permeate side.

Fig.26 shows the concentration gradient present in the tubular membrane module for $CO_2$. The important parameter the arrow shows is the feed gas passes through tube

side to the permeate shell side of the module. The tube surface acts as a membrane which is permeability and selectivity are applied. The results verify that the gradient is present and gas can be diffused through the membrane.

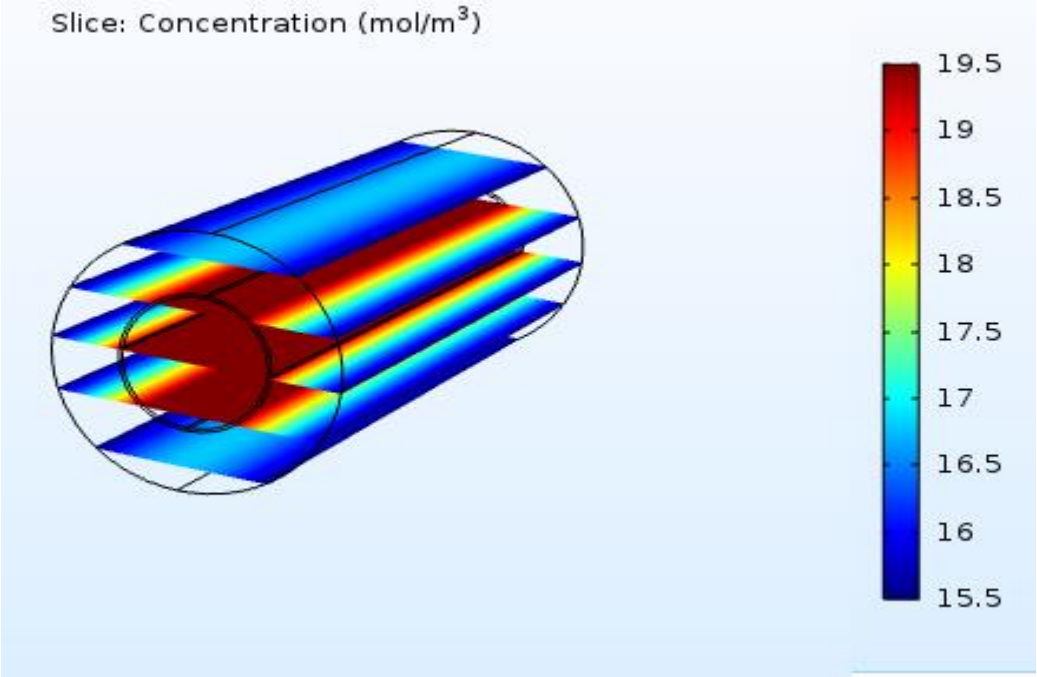


Figure 25: Concentration of $CO_2$ gas in spiral wound membrane module

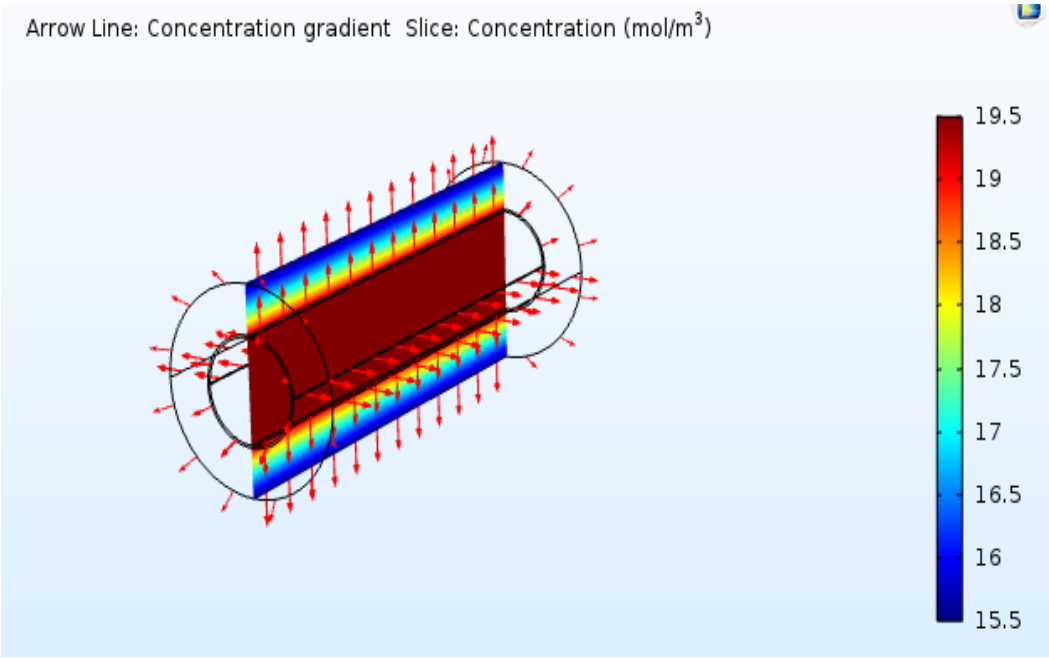


Figure 26: Concentration gradient in spiral wound membrane module

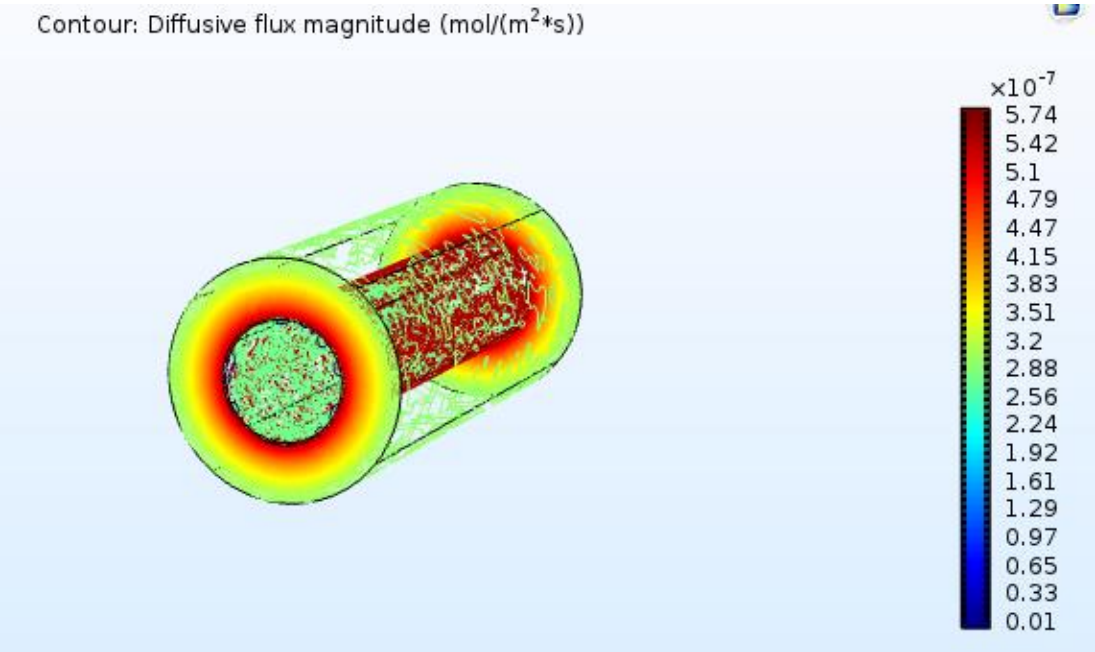


Fig 27: Diffusive flux magnitude in tubular membrane module

The diffusive flux is also present in the tubular membrane module. The result shown in Fig.27 describes the diffusive flux due to diffusion. The flux can be calculated with given parameters to the membrane module. Fig.27 shows the diffusive flux magnitude. The contour displays the flux variations in the tubular membrane module. The colour bar shows the flux magnitude in the module. Basically, the flux is calculated in the module is described by Fick's law.

### 4.4 Flat Sheet Membrane Module

The simplest type of membrane module is flat sheet membrane module in which single sheet of membrane is placed in the centre of the module. The flat sheet membrane module is usually used for the pilot plant testing or lab scale testing. The separation of methane-ethane is considered for flat sheet membrane module. The membrane dimensions are taken from the published literature. The conditions are given in the table 6.

Table 6: Flat Sheet membrane module configuration and specification [31].

| Parameters | Units | Values |
|---|---|---|
| Feed Pressure | Kpa | 103.7 |
| Permeate Pressure | Kpa | 1.01 |

| | | |
|---|---|---|
| Feed Composition | Mol/ m3 | 39.5% |
| Permeance | $m^3/m^2.Pa.s$ | $2\times10^{-7}$ |
| Thickness | M | $15\times10^{-6}$ |
| Effective Area | $m^2$ | 0.3 |

The simulation of flat sheet membrane module was performed to check the concentration change in reject and permeate side. The feed gas entered in the membrane module and permeate was collected at the bottom of the module. The cross-flow model is applied to consider the boundary conditions. The boundary conditions are applied for high feed concentration on right side and low feed concentration on left side. Fig.28 shows the concentration variation in flat sheet membrane module.

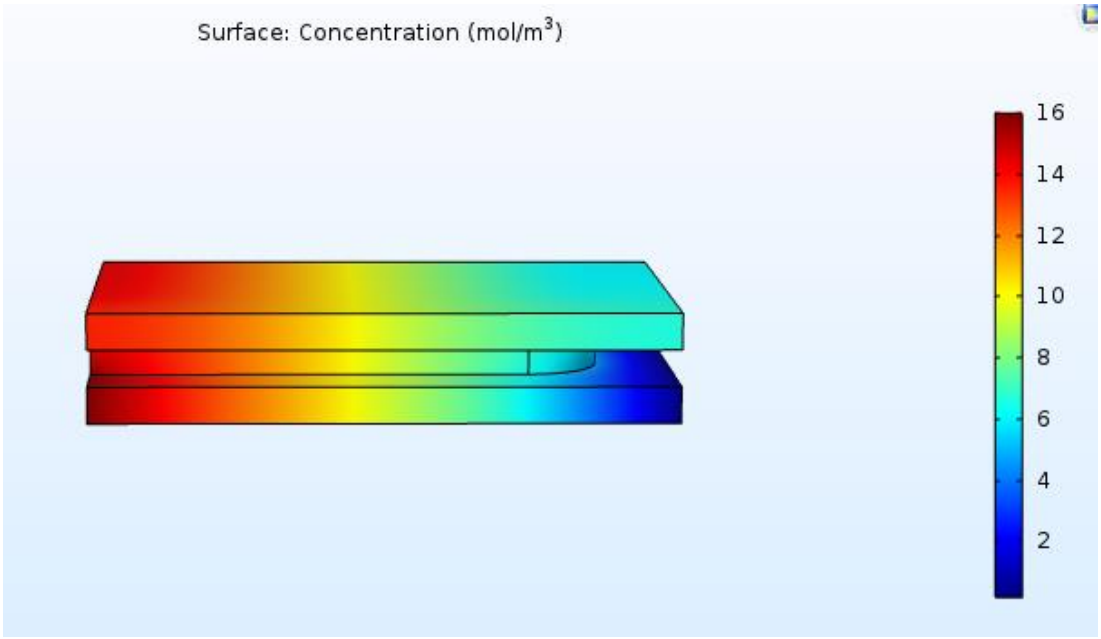


Figure 28: $CH_4$ concentration in Flat Sheet Membrane Module

Fig.28 of flat sheet membrane module shows a concentration of $CH_4$ in feed and permeates side. The applied model is a cross-flow model for gas separation. The contour tells about the concentration variation of gas on both sides of the membrane.

Fig.30 shows that concentration gradient present in the flat sheet membrane module for $CH_4$. The important parameter that arrow shows is the feed gas variation in

permeate and reject side. The membrane is present in the center of the module and permeate is collected at the bottom surface. The results verify that the gradient is present and gas diffuses through the membrane.

The flux can be calculated with given parameters to the software. The contour displays the flux variations in the flat sheet membrane module. The colour bar shows the flux magnitude in the module. Basically, the flux is calculated in the module is described by Fick's law.

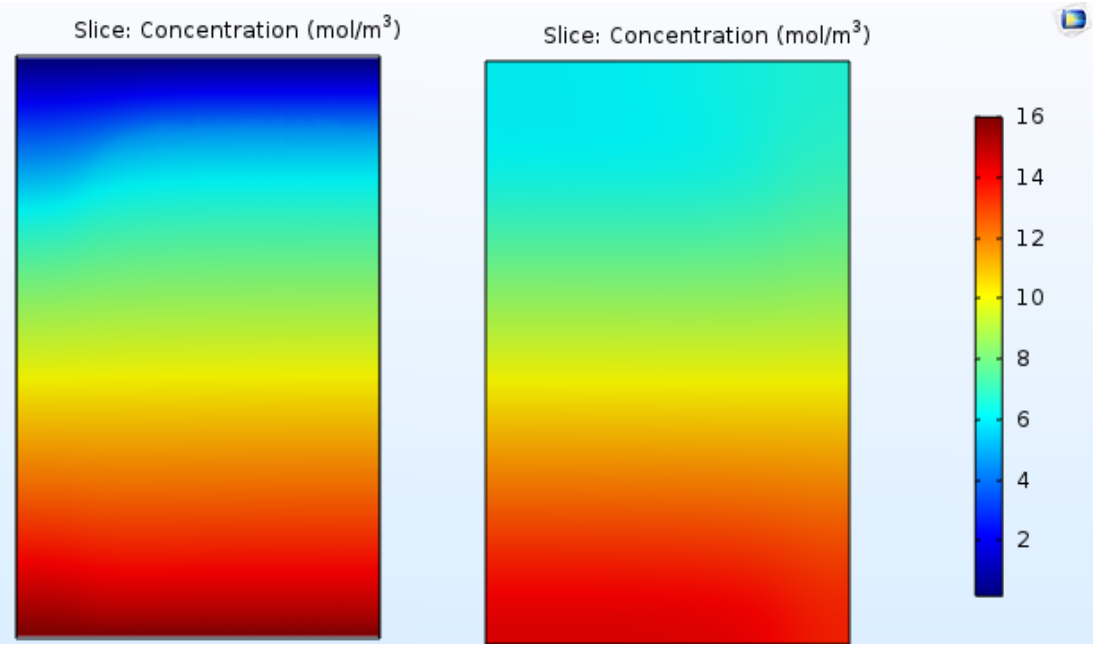


Figure 29: Slice concentration of $CH_4$ in flat sheet membrane module

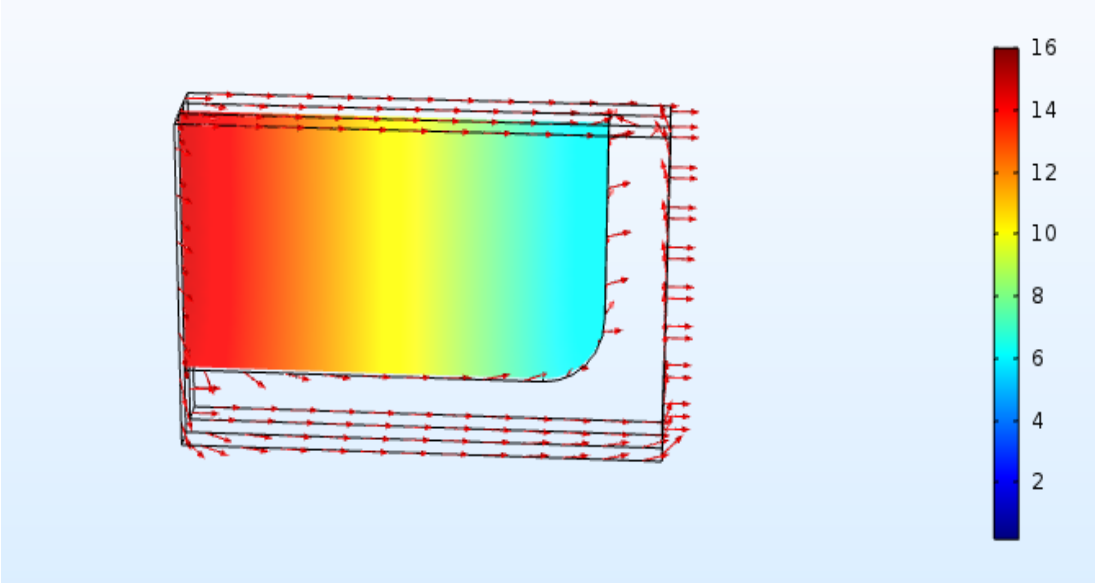


Figure 30 : Concentration gradient in flat sheet membrane module

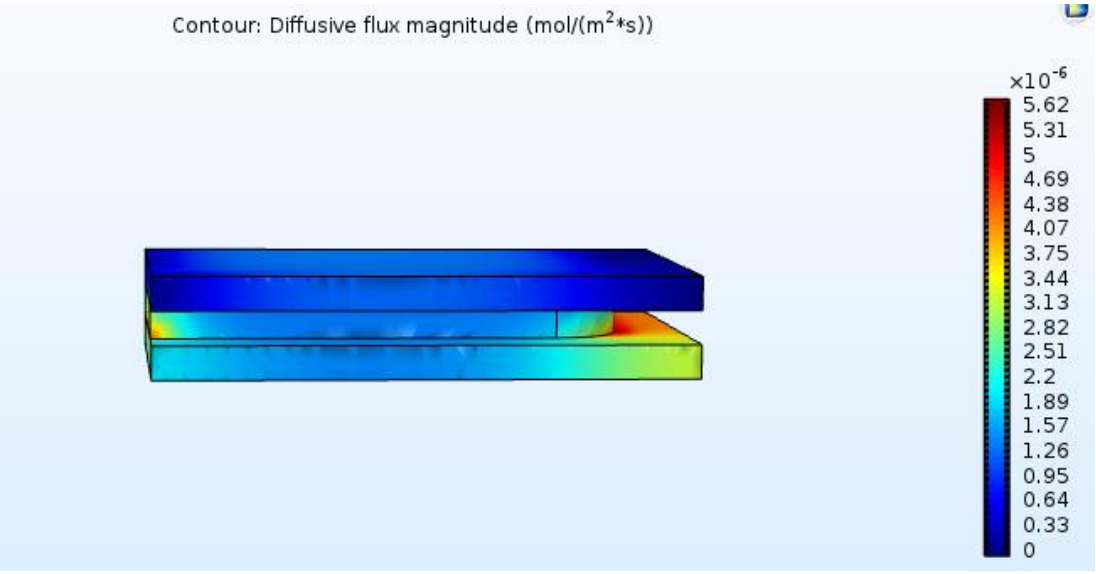


Figure 31: Diffusive flux and total flux in flat sheet membrane module

### 4.4 Parametric Study and Results Validations

#### 4.4.1 Effects on hollow fiber Membrane Module

The hollow fiber membrane module performance was investigated through different parameters like active fiber length, pressure and concentration. The length of module was changed from 5 to 20 cm while the other parameters were kept constant. Fig.32 depicts the simulation results of $O_2/N_2$ separation. The corresponding values were obtained from the simulation at different conditions.

The results obtained from simulations show that the length of fiber increases from 5 to 25 cm then the purity of $O_2$ in permeates decrease from 15% and the concentration of $N_2$ in reject increase almost 10 percent. The length of fiber produces a large membrane area which is used for separation. The higher stage cut is also causing to more gas permeate through the membrane because the extension in length is gradually diluted the permeate stream with $N_2$. Due to this, the $O_2$ goes through in less quantity while the concentration of $N_2$ increases in permeates. Therefore, the purity of permeate side decreases. The oxygen depletion from feed is less enriched than permeate side when high stage cuts are achieved. The simulations results have been compared with literature data and high purities of $O_2$ and $N_2$ obtained in permeate and reject side.

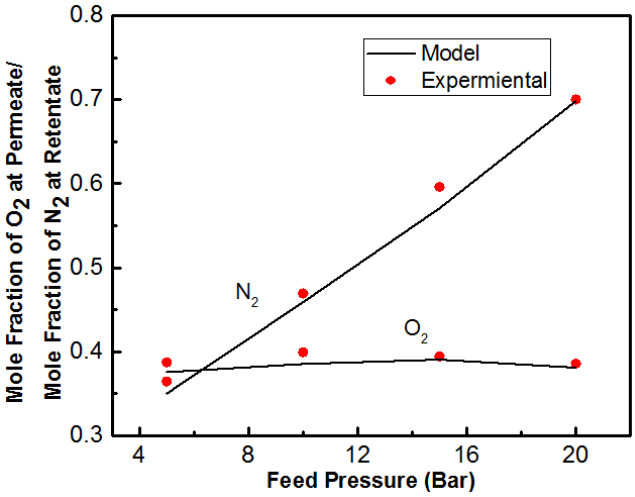


Figure 32: Effect of fiber length on mole fraction of $O_2$/ $N_2$ in permeate and reject side in hollow fiber membrane module

The concentration effect was investigated by changing the values of $O_2$ concentration in the feed, although other parameters were kept constant. The analysis of feed concentration is shown in Fig.33 which shows the concentration of $O_2$ and $N_2$ in permeate and reject side.

The results verified that the increase the concentration of $O_2$ in feed side also gives more permeate at the end. The increase in $O_2$ concentration in feed produces more concentration gradient while gradient for $N_2$ reduces. For long fiber, the lower $O_2$ and higher $N_2$ purities are obtained at any specified feed concentration. The purity of $O_2$ in permeate and $N_2$ in reject streams as a function of mole fraction of $O_2$ in feed at different active fiber lengths are represented in Fig.33.

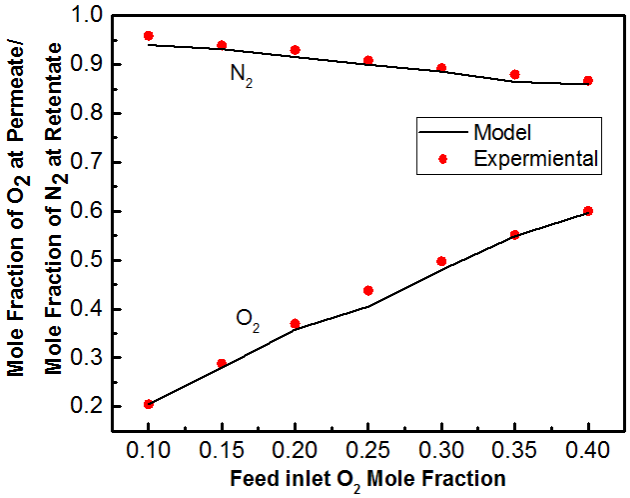

Figure 33: Feed Content effect on the $O_2/N_2$ mole fraction in permeate and reject in hollow fiber membrane module

The pressure effect on the hollow fiber membrane was also investigated by changing the feed pressure from 5 to 25 bar. It was observed that increasing feed pressure gives different behaviour for $O_2$ at permeating outlet while $N_2$ at reject outlet. Fig.34 depicts the effect of feed pressure on the concentration of $O_2$ and $N_2$ at the permeate and reject outlet. It has been a review that the feed pressure increase gives higher permeate concentration of $O_2$. While further increase in the feed pressure reduces the $O_2$ in permeate.

Increase in the feed pressure also produces excessive mass transfer gradient for $N_2$ to pass through from membrane which reduces the concentration of $O_2$ in permeate. Furthermore, it was also observed that maximum purity of product can be achieved at long fiber length with low feed pressure. It is due to the available area for permeation is increased which gives high state cuts and low $O_2$ purity.

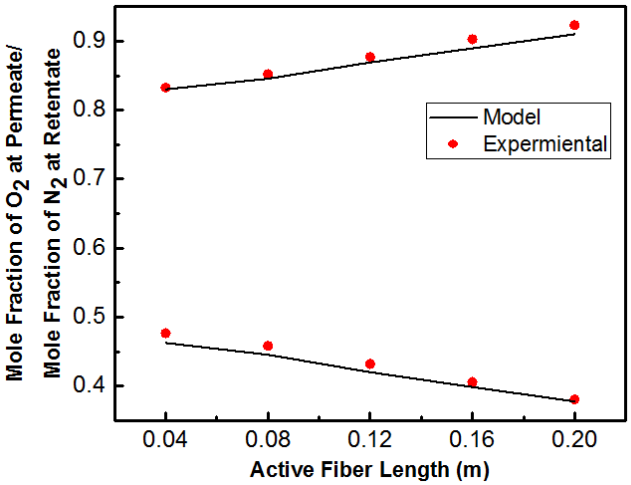


Figure 34: Feed pressure effect on the $O_2/N_2$ mole fraction in permeates and reject in hollow fiber membrane module

Fig.34 shows feed pressure effect on the $O_2/N_2$ mole fraction in permeates and reject in hollow fiber membrane module. The permeation system and chosen operating conditions in counter-current flow pattern give lowest permeate pressure build up. The feed gas enters the tube as counter-current flow pattern in tube bundle with a high concentration of helium. On the other hand, the co-current flow pattern yields a high permeate pressure.

The verified results show that the concurrent patterns give high permeate pressure build up which is enhanced than from cross flow pattern. It mainly happens due to satisfactory feed flow direction with permeate pressure build up.

### 4.4.2 Effects on spiral wound membrane module

The membrane length is considered for spiral wound membrane module and results are verified with literature. Fig.35 shows that the permeate pressure is a function of membrane length for different permeation values. The obtained results show the permeate pressure variation. Increase in membrane modules length always decreases the permeate pressure because gradient at the end of the membrane is small, therefore, less mass transfer occurs then permeate pressure is also decreased.

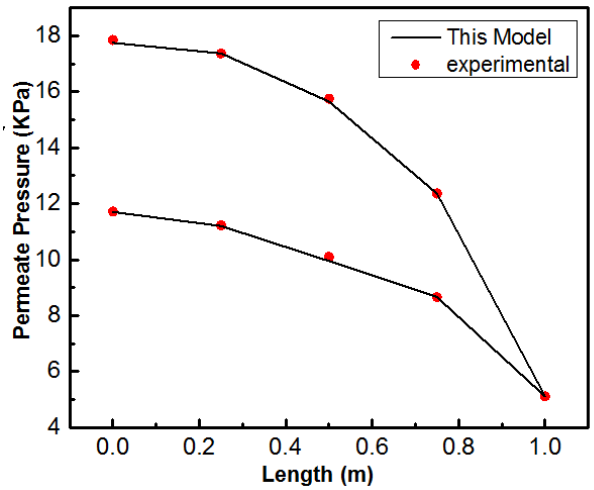


Figure 35: Permeate pressure effect on the membrane length in spiral wound membrane module

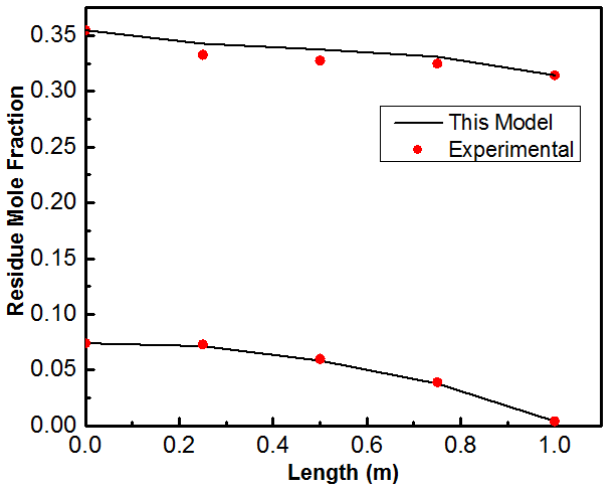

Figure 36: Reject concentration effect on the membrane length in spiral wound membrane module

Fig.36 shows that the residue mole fraction of $CO_2$ changes across the membrane length. The $CO_2$ enters the membrane module through the central tube and is collected at the end of the module. The gas moves in feed channel which is wrapped around the central tube and membrane is placed in the center of feed and permeate channel. The gas diffuses through membrane and residue mole fraction changes with the length of the membrane.

### 4.4.3 Effects on tubular membrane module

It is verified through the obtained simulation results that the methane losses in the tubular membrane module. It is important to notice that methane loss is a percentage of methane lost in permeate side to methane present in feed side. The results show that different parameters for membrane module i.e. fiber length, the outer diameter of the module and the radius of the fiber bundle are verified with the experimental results available in the literature.

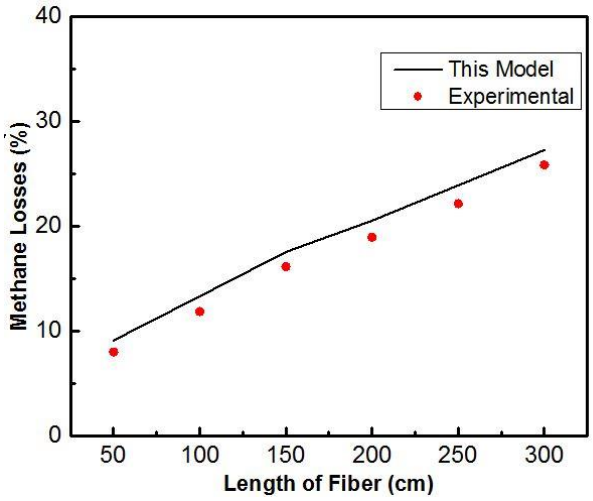


Figure 37: Fiber length effect on methane loss in tubular membrane module

The increase in fiber length results in more $CH_4$ losses because increased fiber length provides more membrane area for separation. Therefore, the higher permeation gives more methane loss. The fiber radius also increased membrane area which also results in more methane loss in the feed stream.

Fig.38 shows that increase in the membrane module diameter tends to decrease the concentration of $CH_4$. It is due to increasing the outer diameter while other

parameters are constant. Therefore, it will result in decreased membrane area. The membrane area reduction will also reduce the permeation through the membrane and results in less methane loss.

These outcomes demonstrate that module features effect a change in the membrane separation area. The increase in membrane area also increases the concentration of $CO_2$ passed through the membrane, gives a high stage cut and vice versa.

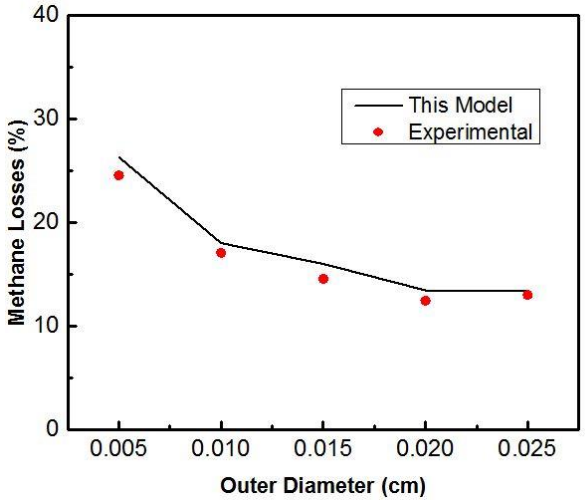


Figure 38: Outer Module diameter effect on methane loss in tubular membrane module

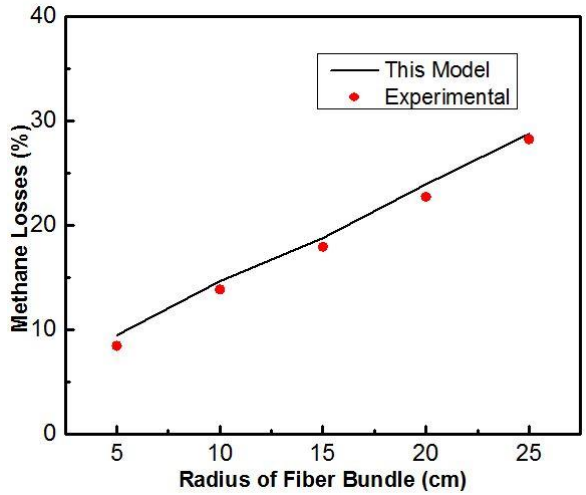


Figure 39: Effect of fiber bundle radius on methane loss in tubular membrane module

### 4.4.4 Effect on flat sheet membrane module

Chan and Yang presented steady-state fluxes of diffusion of single and binary components in 1994. The results have been validated with the fluxes of permeation present in literature. The modeling of membrane module has been performed computationally and obtained results have been verified with experimental results of Chen and Yang.

The carbon membrane is considered as flat sheet membrane in the model. Fig. 40 shows the comparison of modeling results with experimental data. The change in error is below 4 percent.

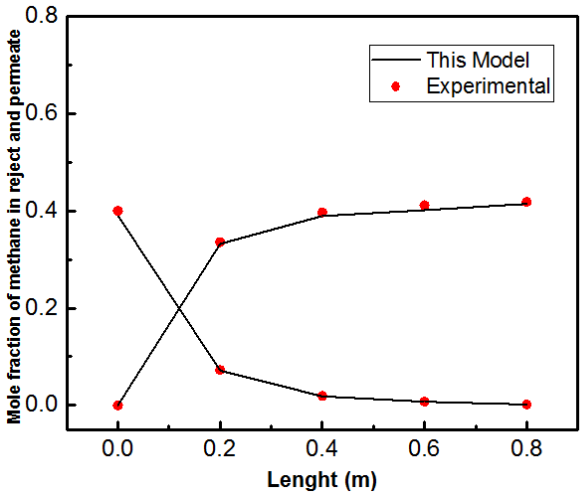


Figure 40 : Effect of length of methane mole fraction in permeate and reject side in flat sheet membrane module

The length is important parameter in the flat sheet membrane module and it was observed that the permeate concentration changes through the length. The permeable component passed through the membrane while other component left as reject. The $CH_4$ gas is more suitable for permeation through the membrane. Fig.40 shows the mole fraction of $CH_4$ increased in permeate side across the length of module and decreased in the reject with respect to length. The ethane gas increased in the reject side because the permeation through the membrane of ethane is very low. Therefore, maximum purity of gases on both sides of the module was achieved.

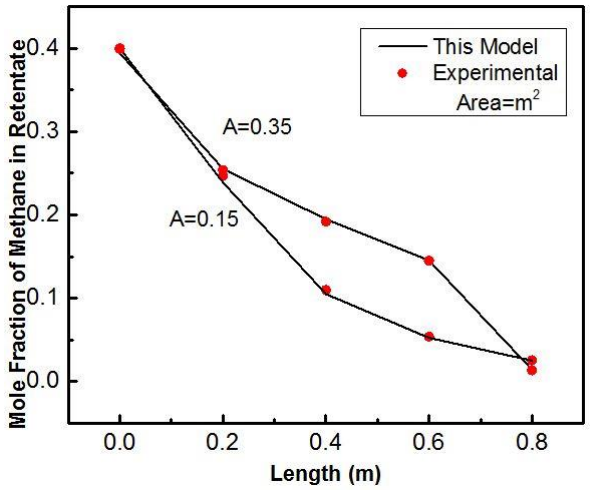


Figure 41 : Membrane area effect on methane mole fraction in reject side in flat sheet membrane module

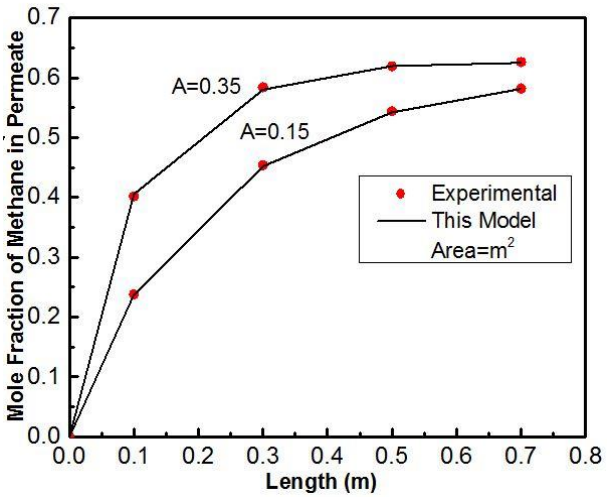


Figure 42 : Membrane area effect on methane mole fraction in permeate side in flat sheet membrane module

Fig.41 and 42 shows the effect of membrane area along the membrane length in flat sheet membrane module. The performance of separation depends on the area, when the membrane effective area is increased the mole fraction of both components decreased in reject side. Increasing the membrane area increases the methane concentration on permeate side. The concentration of methane becomes higher as compared to ethane. As it can be observed in Fig. 42, increasing the membrane area benefits the separation and increases the methane recovery in the permeate side of the module.

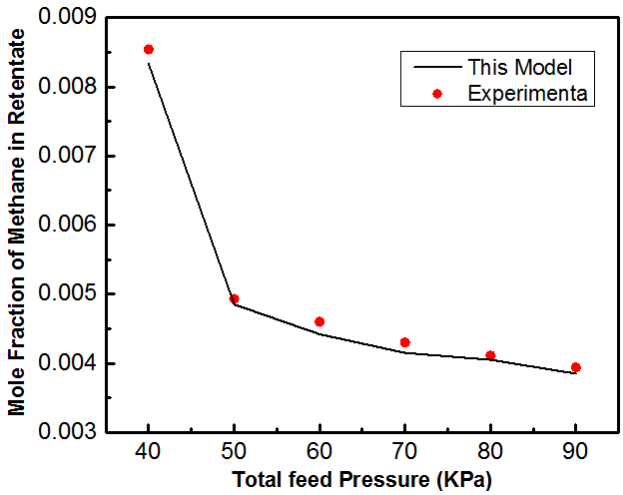


Figure 43 : Feed pressure effect on methane in reject side in flat sheet membrane module

The permeation of components through the membrane increases when driving force is increased. By increasing the feed pressure, the driving force of permeation through the membrane is also increased. Therefore, it is estimated that higher the feed pressure better the separation. It is also better for the methane recovery in the permeate side because increased feed pressure creates more pressure gradient and turbulence for mass transfer, therefore, gas passes through membrane more rapidly. Fig.43 and 44 show that the variations in feed pressure give more purity in permeate and reject side.

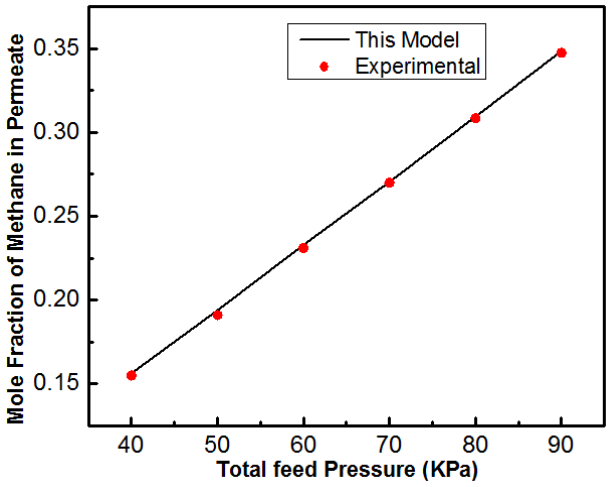


Figure 44 : Feed pressure effect on methane in permeate side in flat sheet membrane module

# Chapter-5

# 5 Using MATLAB NUMERICAL ANALYSIS of HOLLOW FIBER MEMBRANE MODULE

## 5.1 Abstract

An approximated technique for predicting the membrane-based gas separation performance of a separator with asymmetric membranes is proposed. The permeation behaviour of the high-flux asymmetric membrane varies from that of the traditional symmetric membrane. The advanced mathematical model has been applied in this study for the separation of a binary gas mixture. In the present work, a shell-fed hollow fiber module like counter-current flow pattern is modeled mathematically for $CO_2$ separation from $CH_4$. Finite Difference method (FDM) is applied to solving the equations numerically. The models offered separation for a membrane module, for given gas conditions, simulating permeate and residue composition and the stage cut. The different parameters are investigating like change the pressure ratio, stage cut and feed flow rates. The approach is helpful as it entails the least effort and computational time due to the fact algebraic equations are used instead of differential equations. The obtained models data verified with present differential model data and available experimental results.

## 5.2 Introduction

The increase of industries has resulted in rising carbon dioxide in the climate[32]. The environment issues have been held due to globally temperature boost. More than fifty percent of carbon dioxide is produced by power industries and also form non-renewable energy sources[33]. Carbon dioxide which is discharged from petroleum derivative, regular and refinery off gasses and numerous different sources are speaking to around 80% of nursery gasses from the worldwide environmental point of view. The current carbon dioxide separation method as based on physical and chemical strategies including absorption, adsorption and other unit operation like membrane technologies[34, 35]. Therefore, improvement of carbon dioxide from

substantial discharge sources is an impressively innovative and logical test which has gotten extensive consideration for quite a while[33, 36]. However, membrane technology is getting extra regularly used for separation of huge various fuel mixtures in different industries due to the profitable competition of the present separation technology and the present demanding situations of economic environments[3].

Membrane-based gas separation is an effective replacement for common unit operations because of its operational ease, financial viability, low upkeep, small length and low energy consumption[37]. A hollow fiber or spiral wound module is used for gas separation through selective nonporous membrane[38]. Membrane gas separation has used alternative processes like adsorption and absorption and many others. Membrane process plays a vital role in industrial processes such as nitrogen purification, Oxygen recovery, sweetening of natural gas, hydrogen recovery from steam reforming process, carbon dioxide removal from methane[39, 40]. Hollow fiber membrane has numerous advantages like the area to volume ratio, high packing density, and also gives the desired mechanical strength to membrane module, mechanical stability and also reduced resistance from fouling. Hollow fiber membranes are the cheapest membranes which don't require any material as support[41].

Hollow fiber membrane can be of two geometries, shell-side feed and bore side feed. Shell-side feed consists of fibers in a close bundle within a pressure vessel. Pressure is created from the shell-side while through the fiber wall permeation occurs. However, the reject passes through open fiber ends. The design allows the large surface area of membrane material to be compactly enclosed in an economic system. The fiber has small diameters, and the wall has high thickness because of large pressure requirement. The Diameters are in the range of 50 um for internal diameter and 100 – 200 um for outer diameters[42, 43].

Fibers are of open ends and feed fluid circulated through the bore of fibers. The diameters are usually large than those in shell-side feed system thus to minimize the pressure drop. These capillary fibers are used in evaporation, ultrafiltration and gas separation. In this module, feed pressure is limited to 150 psig. The Diameters of all

the fiber have same in bore side feed modules. There is small variation can lead to change the performance of module[42].

The many advantages of hollow fiber membrane are; it can be manufactured by any method to produce a chemical fiber. The highest area to volume ratio makes hollow fibers are cheapest and easily available[41, 44]. Due to its Compact size, it doesn't require any support of material. The module is same as tube heat exchanger and countercurrent shell, but fibers are used as a membrane. To enhance the performance of membrane gas separation and investigation of the procedure should be proficient. These targets are achieved in the using the modeling and simulations techniques[45]. The issue of scientific demonstrating of membrane gas separation was first tended to by Weller& Steiner. Boucif developed mathematical models that show a highly nonlinear behaviour. The boundary value problem experienced in a hollow fiber module with permeates flows in the co-current and counter-current flow with no axial pressure drop. Chern builds a model for binary gas mixture with an isothermal operation. A developed equations were solved as a boundary value problem[46]. Rautenbach & Dahm developed a model with the constant pressure of permeate along the length solved equations numerically for binary gas mixture in both co-current and counter-current manner[47].

This research work shows that the finite difference method (FDM) is used for findings the solution of asymmetric membranes for the separation of $CO_2$ from $CH_4$. The several flow conditions are investigated in this numerical method. The obtained resulted are compared with the present literature data and series solution. The operating parameters such as feed pressure, Permeate pressure, stage cut and the mole fractions of permeate and reject are studied[39]. The purity of desired gas is achieved at a specific level. Commonly, the module configuration is important for the membrane gas separation and also a complicated relationship between model equations gives feasible process and design conditions. This model gives valuable and economical results for the separation of the binary gas mixture.

### 5.3 Mathematical Modeling of Counter-Current flow

Consider a binary gas mixture for the separation through the membrane, where a selectivity of a single component is needed. The permeate composition does not differs from the bulk permeate composition because in asymmetric membranes no

support material is used, but bulk values are considered an average of two local permeate values. This model is solved basically algebraic equations in MATLAB and Excel to finds the solution.

In a counter-current-flow pattern, the permeate gas flow in opposite direction of feed gas but in the co-current flow patterns both gases flow in the same direction. The systematic diagram of counter-current model is given below.

The feed enters into a unit with a flow rate $L_f$ and gives two flow rate after the separation from the membrane. The permeate flow rate $V_p$ collected at the opposite direction of reject flowrate $L_o$ .

The mass balance of the system is

$$L_f = L_o + V_p \quad (1)$$

The stage cut of the system is

$$\theta = \frac{V_p}{L_f} \quad (2)$$

Selectivity is defined as a ratio of Permeability of component A and component B.

$$\alpha = \frac{P'_A}{P'_B} \quad (3)$$

The finite difference model is based on the following assumptions[39].

Model is considered as plug flow.

Assume system is steady state.

The thickness of the membrane is considered as uniform.

The permeability of pure component is kept constant.

The pressure effects of the hollow fiber are negligible.

Concentration gradients in the radial direction have no effect.

The permeance of the system is constant at given temperature.

In a finite difference method, the permeate composition $y_p$ can be calculated form this equation

$$y_p = \frac{-b \pm \sqrt{b^2 - 4ac}}{2a} \quad (4)$$

Where a, b and c are the constants that relate the relationship between selectivity $\alpha^*$ and pressure ratio $r$.

$$a = 1 - \alpha^* \quad (5)$$

$$b = -1 + \alpha^* + \frac{1}{r} + \frac{x_o}{r}(\alpha^* - 1) \quad (6)$$

$$c = \frac{-a * x_o}{r} \quad (7)$$

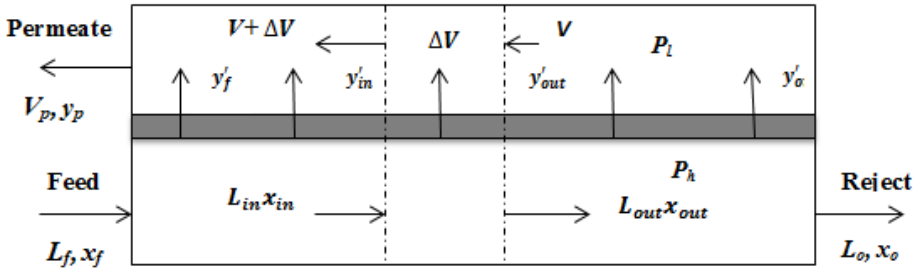


Figure 45: Counter-current flow model

The counter-current model flow diagram shown in Fig 1.Using FDM and mass balance on both streams with the incremental area $\Delta A_m$.

$$\Delta V = L_{in} - L_{out} \quad (9)$$

Where $L_{in}$ and $L_{out}$ are the flow are rates of entering and leaving the system and $\Delta V$ is the permeate flow rate.

$$\Delta V y'_{av} = L_{in} x_{in} - L_{out} x_{out} \quad (10)$$

Where $y'_{av} = (y'_{in} + y'_{out})/2$ .Putting $L_{out}$ from equation (9) into (10)

$$\Delta V = \frac{L_{in}(x_{in} - x_{out})}{y'_{av} - x_{out}} \quad (11)$$

Using equations (4), (10) and (11) have numerically solved with starts at the feed $x_f = x_{in}$ to finds permeate for each specie $\Delta V$ and $y'_{av}$ is calculated for each $\Delta A_m$ to start x to xo at the rentantate and the bulk composition $y_p$ as a function of x and the starting the calculations at xo.

The Equation (12) and (13) and adding $\Delta V$ to obtained the V and $y_p$ is calculated at the feed inlet $x_f$ for each increment $\Delta A_m$.

$$V=\sum \Delta V \quad (12)$$

$$y = \frac{\sum y'_{av}\Delta V}{V} \quad (13)$$

For the counter-current flow area can be calculated as

$$\frac{\Delta V\, y'_{av}}{\Delta A_m} = \frac{\Delta V_A}{\Delta A_m} = \left(\frac{P'_A}{t}\right) * p_h * (x - r'_y) \quad (14)$$

$$r = p_l/p_h$$

Where r is a pressure ratio of feed pressure to the permeate pressure

The average force of driving is

$$(x - r'_y)av = [(x_{in} - ry'_{in}) + (x_{out} - ry'_{out})]/2 \quad (15)$$

To calculated for $\Delta A_m$,

$$\Delta A_m = \frac{\Delta V y'_{av}}{\left(\frac{P'_A}{t}\right) * p_h * (x - r'_y)av} \quad (16)$$

The calculation is starting from $x_f$ for obtaining the $\sum \Delta A_m$ [48].

### 5.4 Results and Discussions

#### 5.4.1 Effect of Feed and Permeate Pressure

Fig 2 shows that increasing the feed pressure will be decreasing the concentration profile of $CO_2$ in reject stream for counter-current flow pattern. By increasing feed pressure, the concentration of $CO_2$ will be decreasing. Due to continuing increases in feed pressure, the rate of mass transfer is increased, and then the purity of $C0_2$ increased in the permeate side. $CO_2$ values are decreasing on the reject side because more $CO_2$ permeate through the membrane. The mole fraction of $CH_4$ is increased on the reject side because mole fraction of $CO_2$ is continuously permeated through the membrane. The increase in feed pressure has the best effect for $CH_4$ because the rate of mass transfer raised, and $CO_2$ more permeate therefore the concentration of $CH_4$ is also increased on the reject side.

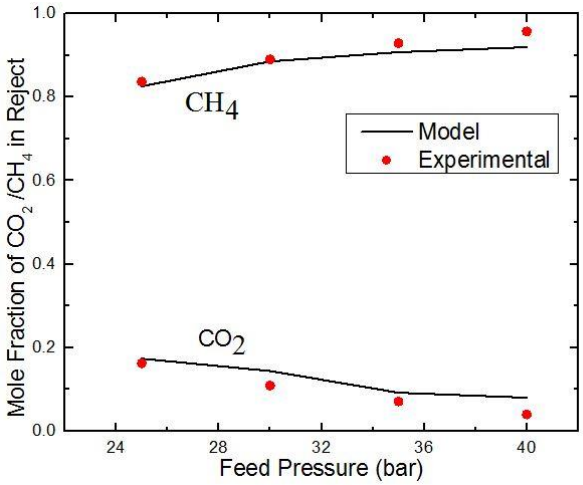


Figure 46: Concentration profiles of $CO_2$ and $CH_4$ in reject with feed pressure for counter-current flow pattern.

For counter-current membrane unit design, permeate pressure is a very important parameter. Fig 3 shows that increases permeate pressure slightly increases the mole fraction of $CO_2$.The concentration of $C0_2$ in reject is increased due to a reduction in the gradient for counter-current Due to permeate pressure increased and less $CO_2$ is passed through the membrane. The mole fraction of $CH_4$ is decreased when increasing the permeate pressure. The behaviour of $CH_4$ is observed opposite due to enhancing the permeate pressure will create a less mass transfer and low $CO_2$ transfer through the membrane. Therefore, purity of $CH_4$ in reject side is decreased.

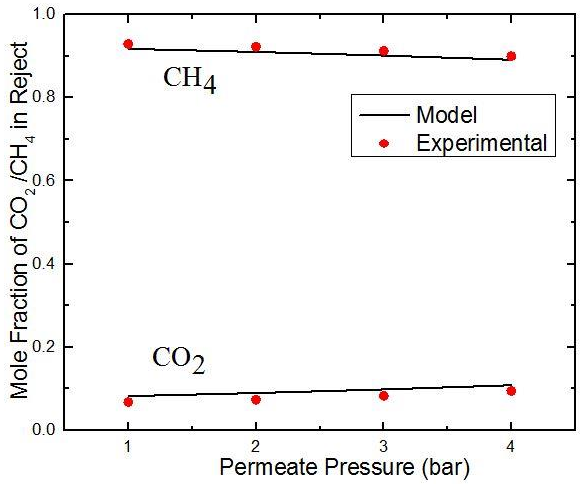


Figure 47: Concentration profiles of $CO_2$ and $CH_4$ on reject side with permeate pressure for counter-current flow pattern.

### 5.4.2 Effect of feed flow rate

The feed flow rate has a greater effect on moles of $CO_2$ on the reject side. The influence of feed flow rate on the counter-current pattern is shown in Fig 4. By increases the feed flow rate, the contact time is $CO_2$ concentration with the membrane active surface area is small then the concentration of $CO_2$ in the permeate side is decreased. Therefore, at a higher flow rate, the concentration of $C0_2$ is increased in the reject. The increasing the feed flow will also affect the purity of $CH_4$ in the reject side. The main theme of this research is achieving higher purity of $CH_4$ in the reject but when increasing the feed flow rate increases the $CO_2$ concentration on the reject side and decreases the concentration of $CH_4$. In Fig 4 shows that the concentration of $CH_4$ is decreasing with increases the feed flow rate.

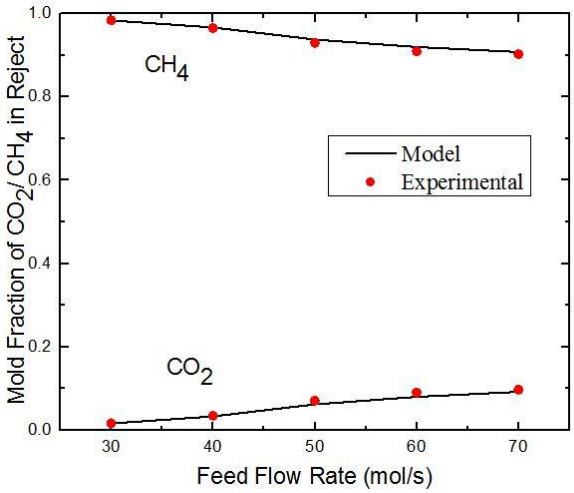


Figure 48: Concentration profiles of $CO_2$ and $CH_4$ in the reject with feed flow rate for counter-current flow pattern.

### 5.4.3 Effect of $CO_2$ concentration in the feed

The feed gas is the key parameter for membrane separation process for counter-current flow percentage of impurities. The feed concentration required a specific area to permeate one component through the membrane. When increasing the feed concentration of $CO_2$ then the amount of gas diffuses through the membrane is decreased due to less area. Fig 5 shows that increases the feed $CO_2$ concentration in feed leads to increases the $CO_2$ concentration in the reject side and decreasing the concentration of $CH_4$ on the reject side.

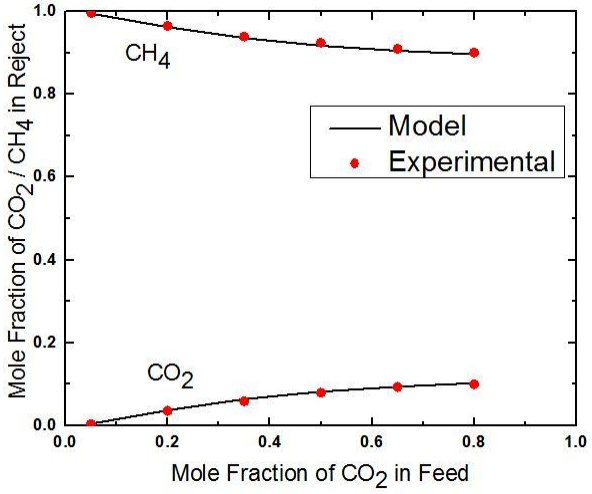


Figure 49: Concentration profiles of $CO_2$ and $CH_4$ in the reject with $CO_2$ feed content for counter-current flow pattern.

Table 7: Percentage errors with experimental results

| Feed Flow rate (mol/s) | Permeate Concentration | Reject Concentration | | |
|---|---|---|---|---|
| | | Arabi | This Model | %change |
| 70 | 0.9178 | 0.0902 | 0.09736 | 5.82 |
| 60 | 0.9106 | 0.08 | 0.0853 | 7.13 |
| 50 | 0.9008 | 0.062 | 0.068 | 4.56 |
| 40 | 0.8886 | 0.033 | 0.03467 | 5.06 |
| 30 | 0.8786 | 0.0166 | 0.01667 | 3.75 |

The table 7 shows the performance of hollow fiber module like counter current flow patterns for different flow rates and reject concentration. The flow rate as a function of stage cut has been investigated for counter-current flow pattern. The data for the performance of asymmetric membranes can be obtained from the mathematical model show in table 1. In table 1, the obtained results from our model compared with available literature data for separation of $CO_2$ from $CH_4$. The results show the better performance of hollow fiber membrane module for the separation of binary gas mixture. The error in data occurred due to the different model equation are used for

the calculations of counter-current flow pattern. The obtain results better for high flow rates because it gives maximum permeation of gas. The increase in high flows rate observed 3% better results in reject values is better than available literature values.

# Chapter-6

# 6 Conclusion

The Computational fluid dynamics simulations have been conducted to study the mass transport in different membrane modules i.e. hollow fiber, spiral wound, tubular and flat sheet membrane module. The three-dimensional geometries have been considered to discuss the membrane-based gas separation for the binary gas mixture. The counter-current and cross-flow membrane model is applied to verify the results. The Fick's law was applied to describe the mass flux transport through the membrane for the binary gas mixture. The membrane model was defined in COMSOL Multiphysics software for the separation of the binary mixture. The membrane model was applied as a thin diffusion barrier which allows certain species to pass through the membrane. The effect of molar flux for species has been considered in mass transport through the membrane. Different gas mixtures like $CO_2/CH_4$, $O_2/N_2$ and $CH_4/C_2H_6$ were investigated in different membrane modules. In hollow fiber membrane module, the $O_2/N_2$ separation through membrane was investigated.

The membrane model was developed using COMSOL MULTIPHYSICS. Different module geometries were developed for the flat sheet. Spiral wound, tubular and hollow fiber membrane modules for further study. The concentration polarization was studies in the membrane modules considering different parameters such as feed pressure, module length, permeate pressure and feed concentration etc. Different gas mixtures were used for different modules in consideration of the available literature data for further validation and comparative analysis.

It was observed and concluded that in flat sheet membrane module with increasing feed pressure the pressure gradient also increased which resulted in higher flux, higher permeation and maximum purity of the permeate. The concentration polarization was observed to be negligible. Further, with increasing module length in flats sheet membrane module, a decrease in concentration polarization was observed because increase in the module length resulted in more permeation of desired component and increase in permeate purity. In spiral would membrane module the

increase in membrane length showed considerable decrease in the concentration polarization. When the length of the membrane was increased, an increase in the residue mole fraction was observed; an increase in the permeate purity was also observed, which indicated that the concentration polarization was negligible. In tubular membranes it was observed that with increase in fiber radius the area increases which results in higher permeation and higher purity of the permeate. Similar effect was observed when length of the fiber was increased. Hence, it can be concluded that in tubular membrane modules, the increase in fiber radius and increase in fiber length decreases the concentration polarization. In hollow fiber membrane module, it was observed that increase in the feed pressure results in the increased pressure gradient, higher flux, more permeability, higher permeate purity, indicating the negligible concentration polarization. Similarly, the increase in feed concentration resulted in increased permeate mole fraction of permeate side excess gradient to facilitate higher permeation and permeate purity. Furthermore, with increase in module length more concentration polarization was observed. Therefore, it can be concluded that in hollow fiber membranes when the feed pressure and feed concentration are increased the concentration polarization decrease while with increase in module length concentration polarization increases.

Furthermore, the applied counter-current model has greater advantages than other differential models; it gave valuable results and required less time to simulate. A model is developed to simulate the membrane-based separation of $CO_2$ from $CH_4$. This model is validated with the present literature data and predicts the values of streams at the different flow rates and other various conditions. The counter-current shows that high permeate efficiency for separation of $CO_2$ from $CH_4$. This pattern is used to finds the effect of different parameters on the separation of $CO_2$ from $CH_4$. It has found that feed pressure, feed flow rate has direct effect and permeate pressure has opposite effect on the purity of $CH_4$ in the reject stream. The membrane area is also increased when increases the permeate pressure but decreases with feed pressure. There are no certain values on used properties of the membrane. Therefore, the study of these parameters is impossible here. The models obtained results are validated using predicting data from the literature for binary gas.

## 6.1 Future Recommendations

The future direction had much more importance on the following topics to describe the flow dynamics of different membrane processes.

- CFD modeling of membrane gas separation for the multicomponent gas mixture.
- Unsteady modeling of membrane modules using different feed spacers and mixer for gas separation

# References


1. Bernardo, P., E. Drioli, and G. Golemme, *Membrane gas separation: a review/state of the art.* Industrial & Engineering Chemistry Research, 2009. **48**(10): p. 4638-4663.
2. Bernardo, P. and G. Clarizia, *30 years of membrane technology for gas separation.* CHEMICAL ENGINEERING, 2013. **32**.
3. Shamsabadi, A.A., et al., *Mathematical modeling of CO2/CH4 separation by hollow fiber membrane module using finite difference method.* Journal of Membrane and Separation Technology, 2012. **1**(1): p. 19-29.
4. Nunes, S.P. and K.-V. Peinemann, *Membrane technology*2001: Wiley Online Library.
5. Chen, W.-H., C.-H. Lin, and Y.-L. Lin, *Flow-field design for improving hydrogen recovery in a palladium membrane tube.* Journal of Membrane Science, 2014. **472**: p. 45-54.
6. Baker, R.W. and B.T. Low, *Gas separation membrane materials: a perspective.* Macromolecules, 2014. **47**(20): p. 6999-7013.
7. Fuertes, A.B. and I. Menendez, *Separation of hydrocarbon gas mixtures using phenolic resin-based carbon membranes.* Separation and purification technology, 2002. **28**(1): p. 29-41.
8. Baker, R.W., *Future directions of membrane gas separation technology.* Industrial & Engineering Chemistry Research, 2002. **41**(6): p. 1393-1411.
9. Rezakazemi, M., et al., *State-of-the-art membrane based CO 2 separation using mixed matrix membranes (MMMs): an overview on current status and future directions.* Progress in Polymer Science, 2014. **39**(5): p. 817-861.
10. Baker, R.W., *Membrane technology and applications.* John Wiley & Sons, Ltd, 2004: p. 96-103.
11. Kesting, R.E. and A. Fritzsche, *Polymeric gas separation membranes*1993: Wiley-Interscience.
12. Li, N.N., et al., *Advanced membrane technology and applications*2011: John Wiley & Sons.
13. Koros, W. and G. Fleming, *Membrane-based gas separation.* Journal of Membrane Science, 1993. **83**(1): p. 1-80.

14. Goh, P., et al., *Recent advances of inorganic fillers in mixed matrix membrane for gas separation.* Separation and purification technology, 2011. **81**(3): p. 243-264.
15. Matsuura, T., *Synthetic membranes and membrane separation processes*1993: CRC press.
16. Mulder, J., *Basic principles of membrane technology*2012: Springer Science & Business Media.
17. Baker, R.W., *Overview of membrane science and technology*. Membrane Technology and Applications, Second Edition, 2004: p. 1-14.
18. Saeed, A., R. Vuthaluru, and H.B. Vuthaluru, *Impact of feed spacer filament spacing on mass transport and fouling propensities of RO membrane surfaces.* Chemical Engineering Communications, 2015. **202**(5): p. 634-646.
19. Mojab, S., et al., *Unsteady laminar to turbulent flow in a spacer-filled channel.* Flow, turbulence and combustion, 2014. **92**(1-2): p. 563-577.
20. Shakaib, M., S. Hasani, and M. Mahmood, *CFD modeling for flow and mass transfer in spacer-obstructed membrane feed channels.* Journal of Membrane Science, 2009. **326**(2): p. 270-284.
21. Koutsou, C.P. and A.J. Karabelas, *A novel retentate spacer geometry for improved spiral wound membrane (SWM) module performance.* Journal of Membrane Science, 2015. **488**: p. 129-142.
22. Karode, S.K. and A. Kumar, *Flow visualization through spacer filled channels by computational fluid dynamics I.: Pressure drop and shear rate calculations for flat sheet geometry.* Journal of Membrane Science, 2001. **193**(1): p. 69-84.
23. Fimbres-Weihs, G. and D. Wiley, *Numerical study of mass transfer in three-dimensional spacer-filled narrow channels with steady flow*. Journal of Membrane Science, 2007. **306**(1): p. 228-243.
24. Vinther, F., et al., *Predicting optimal back-shock times in ultrafiltration hollow fibre modules through path-lines.* Journal of Membrane Science, 2014. **470**: p. 275-293.
25. Marcos, B., et al., *CFD modeling of a transient hollow fiber ultrafiltration system for protein concentration.* Journal of Membrane Science, 2009. **337**(1): p. 136-144.

26. Alrehili, M., et al., *Flows past arrays of hollow fiber membranes–Gas separation.* International Journal of Heat and Mass Transfer, 2016. **97**: p. 400-411.
27. Anqi, A.E., N. Alkhamis, and A. Oztekin, *Computational study of desalination by reverse osmosis—Three-dimensional analyses.* Desalination, 2016. **388**: p. 38-49.
28. Hosseini, S.S., et al., *Simulation and sensitivity analysis of transport in asymmetric hollow fiber membrane permeators for air separation.* RSC Advances, 2015. **5**(105): p. 86359-86370.
29. Qi, R. and M.A. Henson, *Approximate modeling of spiral-wound gas permeators.* Journal of Membrane Science, 1996. **121**(1): p. 11-24.
30. Ahmad, F., et al., *Hollow fiber membrane model for gas separation: Process simulation, experimental validation and module characteristics study.* Journal of Industrial and Engineering Chemistry, 2015. **21**: p. 1246-1257.
31. Gholami, G., M. Soleimani, and M. Takht Ravanchi, *Mathematical Modeling of Gas Separation Process with Flat Carbon Membrane.* Journal of Membrane Science and Research, 2015. **1**(2): p. 90-95.
32. Kanehashi, S., et al., *Membrane gas separation.* 2010.
33. Sohrabi, M.R., et al., *Mathematical modeling and numerical simulation of CO 2 transport through hollow-fiber membranes.* Applied Mathematical Modelling, 2011. **35**(1): p. 174-188.
34. Khoo, H.H. and R.B. Tan, *Life cycle investigation of CO2 recovery and sequestration.* Environmental science & technology, 2006. **40**(12): p. 4016-4024.
35. Ji, P., et al., *Preparation of hollow fiber poly (N, N-dimethylaminoethyl methacrylate)–poly (ethylene glycol methyl ether methyl acrylate)/polysulfone composite membranes for CO 2/N 2 separation.* Journal of Membrane Science, 2009. **342**(1): p. 190-197.
36. Ravanchi, M.T., T. Kaghazchi, and A. Kargari, *Application of membrane separation processes in petrochemical industry: a review.* Desalination, 2009. **235**(1): p. 199-244.
37. Boucif, N., A. Sengupta, and K.K. Sirkar, *Hollow fiber gas permeator with countercurrent or cocurrent flow: series solutions.* Industrial & engineering chemistry fundamentals, 1986. **25**(2): p. 217-228.

38. Pan, C., *Gas separation by high-flux, asymmetric hollow-fiber membrane.* AIChE journal, 1986. **32**(12): p. 2020-2027.
39. Ahsan, M. and A. Hussain, *Mathematical modelling of membrane gas separation using the finite difference method.* Pacific Science Review A: Natural Science and Engineering, 2016. **18**(1): p. 47-52.
40. Kundu, P.K., A. Chakma, and X. Feng, *Effectiveness of membranes and hybrid membrane processes in comparison with absorption using amines for post-combustion CO 2 capture.* International Journal of Greenhouse Gas Control, 2014. **28**: p. 248-256.
41. Antonson, C.R., et al., *Analysis of gas separation by permeation in hollow fibers.* Industrial & Engineering Chemistry Process Design and Development, 1977. **16**(4): p. 463-469.
42. Baker, R.W., *Membrane technology*2000: Wiley Online Library.
43. Basaran, O.A. and S.R. Auvil, *Asymptotic analysis of gas separation by a membrane module.* AIChE journal, 1988. **34**(10): p. 1726-1731.
44. Soni, V., et al., *A general model for membrane-based separation processes.* Computers & Chemical Engineering, 2009. **33**(3): p. 644-659.
45. Tessendorf, S., R. Gani, and M.L. Michelsen, *Modeling, simulation and optimization of membrane-based gas separation systems.* Chemical engineering science, 1999. **54**(7): p. 943-955.
46. Boucif, N., S. Majumdar, and K.K. Sirkar, *Series solutions for a gas permeator with countercurrent and cocurrent flow.* Industrial & engineering chemistry fundamentals, 1984. **23**(4): p. 470-480.
47. Rautenbach, R. and W. Dahm, *Simplified calculation of gas-permeation hollow-fiber modules for the separation of binary mixtures.* Journal of membrane science, 1986. **28**(3): p. 319-327.
48. Geankoplis, C.J., *Transport processes and separation process principles:(includes unit operations)*2003: Prentice Hall Professional Technical Reference.